ผลของเคอร์คูมินต่อภาวะตับอักเสบในหนูไมซ์ที่ได้รับพาราเซตามอลเกินขนาด

นางสาวกาญจนา โสมนวัตร์

วิทยานิพนธ์นี้เป็นส่วนหนึ่งของการศึกษาตามหลักสูตรปริญญาวิทยาศาสตรมหาบัณฑิต
สาขาวิชาวิทยาศาสตร์การแพทย์
คณะแพทยศาสตร์ จุฬาลงกรณ์มหาวิทยาลัย
ปีการศึกษา 2554
ลิขสิทธิ์ของจุฬาลงกรณ์มหาวิทยาลัย

EFFECTS OF CURCUMIN ON HEPATITIS IN MICE WITH PARACETAMOL
OVERDOSE

Miss Kanjana Somanawat

A Thesis Submitted in Partial Fulfillment of the Requirements
for the Degree of Master of Science Program in Medical Science
Faculty of Medicine
Chulalongkorn University
Academic Year 2011
Copyright of Chulalongkorn University

Thesis Title   EFFECTS OF CURCUMIN ON HEPATITIS IN MICE
                    WITH PARACETAMOL OVERDOSE
By   Miss Kanjana Somanawat
Field of Study   Medical Science
Thesis Advisor   Associate Professor Duangporn Thong-Ngam, M.D.

Accepted by the Faculty of Medicine, Chulalongkorn University in Partial Fulfillment of the Requirements for the Master's Degree

……………………………………….. Dean of the Faculty of Medicine

(Associate Professor Sophon Napathorn, M.D.)

THESIS COMMITTEE

……………………………………….. Chairman

(Associate Professor Vilai Chentanez, M.D., Ph.D.)

……………………………………….. Thesis Advisor

(Associate Professor Duangporn Thong-Ngam, M.D.)

……………………………………….. Examiner

(Associate Professor Pisit Tangkijvanich, M.D.)

……………………………………….. Examiner

(Associate Professor Supeecha Wittayalertpanya)

……………………………………….. External Examiner

(Bubpha Pornthisarn, M.D.)

กาญจนา โสมนวัตร์ : ผลของเคอร์คูมินต่อภาวะตับอักเสบในหนูไมซ์ที่ได้รับพารา เซตามอลเกินขนาด. (EFFECTS OF CURCUMIN ON HEPATITIS IN MICE WITH PARACETAMOL OVERDOSE) อ. ที่ปรึกษาวิทยานิพนธ์หลัก : รศ. พญ. ดวงพร ทองงาม, 76 หน้า.

พาราเซตามอล เกินขนาด ถูกเมตาบอลิสมโดยเอนไซม์ไซโตโครมพีโฟร์ฟิบตี้ ทูอีวัน (CYP 2E1) ได้เป็นเอ็นเอพีคิวไอ (NAPQI) เป็นสารพิษจากกระบวนการ เมตาบอลิสมถูกสร้าง ขึ้นในปริมาณมากในที่สุดทำให้เกิดเป็นพิษต่อตับ การ ศึกษานี้เพื่อดูผลของเคอร์คูมินต่อภาวะ ตับอักเสบในหนูไมซ์ที่ได้รับพารา เซตามอลเกินขนาด โดยแบ่งหนูไมซ์เพศผู้ น้ำหนัก 25-30 กรัม ออกเป็น 4 กลุ่ม กลุ่มที่ 1 ป้อนน้ำกลั่นเป็นกลุ่มควบคุม กลุ่มที่ 2 ป้อนพาราเซตามอล 400 มิลลิกรัมต่อกิโลกร ม (มก/กก) กลุ่มที่ 3 ป้อนพาราเซตามอล 400 มก/กก และเคอร์คูมิน 200 มก/กก พร้อมกัน และกลุ่มที่ 4 ป้อนพาราเซตามอล 400 มก/กก และเคอร์คูมิน 600 มก/กก พร้อมกัน หลังจากนั้นเก็บเนื้อเยื่อตับเพื่อวิเคราะห์หาระดับกลูตาไธโอน (GSH) มาลอนไดอัลดี ไฮด์ (MDA) และพยาธิวิทยาชิ้นเนื้อ เก็บซีรั่มเพื่อวิเคราะห์หาระดับเอนไซม์ตับ ระดับ อินเตอร์ ลิวคิน (IL)-12 และ IL-18 ผลการทดลองแสดงให้เห็นว่าทั้งระดับ MDA เอนไซม์ตับ ซี รั่ม IL-12 และ IL-18 เพิ่มสูงขึ้นอย่างมีนัยสำคัญทางสถิติในกลุ่ม หนูที่ได้รับพาราเซตามอล เมื่อ เปรียบเทียบกับกลุ่มควบคุมและค่าเหล่านี้ลดลงอย่างมีนัยสำคัญทางสถิติในกลุ่มที่ได้รับพารา เซตามอล+เคอร์คูมิน 200 มก/กก และพาราเซตามอล +เคอร์คูมิน 600 มก/กก เมื่อเปรียบเทียบ กับกลุ่มที่ได้รับพาราเซตามอล นอกจากนี้พบว่าระดับ GSH ลดลงอย่างมีนัยสำคัญทางสถิติใน กลุ่มที่ ได้รับพาราเซตามอล เมื่อเปรียบเทียบกับกลุ่มควบคุมและ GSH จะเพิ่มขึ้นอย่างมี นัยสำคัญทางสถิติในกลุ่มที่ได้รับพาราเซตามอล+เคอร์คูมิน 200 มก/กก และพาราเซตามอล + เคอร์คูมิน 600 มก/กก เมื่อเปรียบเทียบกับกลุ่มที่ได้รับพาราเซตามอล ดังนั้น สรุปได้ว่าพาราเซ ตามอลเกินขนาดทำให้เกิดความเป็นพิษต่อตับ และเคอร์คูมินสามารถลดการเกิดภาวะ ออกซิเด ทีฟสเตรส ลดตับอักเสบ เพิ่มระดับ GSH และทำให้พยาธิสภาพของตับดีขึ้น นอกจากนี้ เคอร์คู มิน 600 มก/กก มีแนวโน้ม ให้ผลในการลดภาวะต บอักเสบได้ดีกว่าเคอร์คูมิน 200 มก/กก

สาขาวิชา...วิทยาศาสตร์การแพทย์.....   ลายมือชื่อนิสิต...
ปีการศึกษา...2554……………......   ลายมือชื่อ อ.ที่ปรึกษาวิทยานิพนธ์หลัก………….......

5274862430 : MAJOR   MEDICAL SCIENCE
KEYWORDS :   PARACETAMOL / CURCUMIN / OXIDATIVE STRESS / HEPATITIS / GSH / IL-12 / IL-18

KANJANA SOMANAWAT : EFFECTS OF CURCUMIN ON HEPATITIS IN MICE WITH PARACETAMOL OVERDOSE. ADVISOR : ASSOC. PROF. DUANGPORN THONG-NGAM, M.D., 76 pp.

N-acetyl-*p*-aminophenol (APAP) or paracetamol overdose is metabolized by cytochrome P450 (CYP 2E1) and a toxic metabolite, mainly N-acetyl-*p*-benzoquinone imine (NAPQI) is formed, finally, liver injury occurs. Here, we examined the effects of curcumin attenuated hepatitis in mice with APAP overdose. Male mice (25-30 gram) were divided into four groups. Group I (Control); was gavaged with distilled water. Group II (APAP); was gavaged with a single dose of 400 mg/kg APAP dissolve in water. Group III (APAP + CUR 200); was gavaged with a single dose of 400 mg/kg APAP and 200 mg/kg curcumin. Group IV (APAP + CUR 600); was gavaged with a single dose of 400 mg/kg APAP and 600 mg/kg curcumin. The liver was collected for hepatic GSH, hepatic MDA, and liver pathology assays. The serum was collected for hepatic enzymes, IL-12, and IL-18 assays using ELISA technique. Hepatic MDA, hepatic enzymes, serum IL-12, and IL-18 were significantly increased in APAP as compared with control and significantly decreased in APAP + CUR 200 and APAP + CUR 600 as compared with APAP. Hepatic GSH was significantly decreased in APAP as compared with control and significantly increased in APAP + CUR 200 and APAP + CUR 600 as compared with APAP. Liver pathology of APAP showed extensive hemorrhagic hepatic necrosis involving all zones and the improvement of liver pathology revealed in APAP + CUR 200 and APAP + CUR 600. In conclusion, APAP overdose can cause liver injury. The results show that curcumin could attenuate APAP-induced liver injury by decrease oxidative stress, reduce liver inflammation, restoring hepatic GSH, and improve liver pathology. In addition, curcumin at the dose of 600 mg/kg tends to be more potent than 200 mg/kg in preventing the effects of APAP hepatotoxicity. Hence, curcumin might be a novel therapeutic strategy against hepatitis caused by APAP overdose.

Field of Study :…Medical.Science….......   Student's Signature ....

Academic Year :..2011……………....….   Advisor's Signature ....

ACKNOWLEDGEMENTS

CONTENTS

CONTENTS (Continue)

LIST OF TABLES

LIST OF FIGURES

LIST OF FIGURES (Continue)

LIST OF ABBREVIATIONS

APAP	=	N-acetyl-p-aminophenol
ALT	=	Alanine aminotransferase
AST	=	Aspartate aminotransferase
Alpha-KG	=	Alpha- Ketoglutarate
BW	=	Body weight
CUR	=	Curcumin
CYP	=	Cytochrome P450
CLMF	=	Cytotoxic lymphocyte maturation factor
COX-2	=	Cyclooxygenase-2
CCl_4	=	Carbon tetrachloride
DILI	=	Drug-induced liver injury
DTNB	=	5, 5'-dithio-bis-(2-nitrobenzoic acid)
DMSO	=	Dimethylsulfoxide
2, 4 DNPH	=	2, 4 dinitrophenyl hydrazine
ELISA	=	Enzyme-linked immunosorbent assay
GSH	=	Reduced glutathione
GSSG	=	Oxidized glutathione
g/kg	=	Gram per kilogram
H & E	=	Hematoxylin and eosin
H_2O_2	=	Hydrogen peroxide radical
HCl	=	Hydrochloric acid
IL-12	=	Interleukin-12
IL-18	=	Interleukin-18
IFN-γ	=	Interferon-gamma
ICE	=	IL-1 converting enzyme
iNOS	=	Inducible nitric oxide synthase
i.p.	=	Intraperitoneal
KCl	=	Potassium chloride
LDH	=	Lactate dehydrogenase
LM	=	Light microscope
MDH	=	Malate dehydrogenase
mM	=	Millimolar
mg/kg	=	Milligram per kilogram
mL	=	Millilitre
M	=	Molar
μM	=	Micromolar
μL	=	Microlitre
μm	=	Micrometer
mg/day	=	Milligram per day
NAPQI	=	N-acetyl-p-benzoquinone imine
NAC	=	N-acetyl cysteine
NaOH	=	Sodium hydroxide
nmol/mg	=	Nanomole per milligram
nm	=	Nanometer
ng	=	Nanogram

NKSF	=	Natural killer cells stimulatory factor
NK cells	=	Natural killer cells
O.D.	=	Optical density
O_2^-	=	Superoxide radical
PBS	=	Phosphate buffer saline
pg/mL	=	Pictogram per millilitre
r.p.m.	=	Revolution per minute
SDS	=	Sodium dodecyl sulfate
SD	=	Standard deviation
SOD	=	Superoxide dismutase
TBARs	=	Thiobarbituric acid reactive substances
TNF-α	=	Tumor necrosis factor-alpha
Th1	=	T helper type 1
TMP	=	Tetramethoxypropane
TNB	=	5-thio-2-nitrobenzoic acid

CHAPTER I

INTRODUCTION

1.1 Rationale

1.1.1 Drug-induced liver injury (DILI)

Drug-induced liver injury (DILI) is a major health problem that challenges not only health care professionals but also the pharmaceutical industry and drug regulatory agencies (1). According to the United States Acute Liver Failure Study Group (2), DILI accounts for more than 50% of acute liver failure, including hepatotoxicity caused by overdose of N-acetyl-*p*-aminophenol (APAP) or paracetamol (39%) and idiosyncratic liver injury triggered by other drugs (13%). Although the exact mechanism of DILI remains largely unknown, it appears to involve in 2 pathways: direct hepatotoxicity and adverse immune reactions. In most instances, DILI is initiated by the bioactivation of drugs to chemically reactive metabolites, which have the ability to interact with cellular macromolecules such as proteins, lipids, and nucleic acids, leading to protein dysfunction, lipid peroxidation (oxidative stress), and DNA damage. Additionally, these reactive metabolites may induce disruption of ionic gradients and intracellular calcium stores, resulting in mitochondrial dysfunction and loss of energy production. This impairment of cellular functions can culminate in cell death and possible liver failure.

In addition, DILI can affect both parenchymal and nonparenchymal cells of the liver, leading to a wide variety of pathological conditions, including acute and chronic hepatocellular hepatitis (3). The predominant form of DILI is acute hepatitis. Acute hepatitis is defined as a marked increase in aminotransferases or hepatic enzymes, alanine aminotransferase (ALT) and aspartate aminotransferase (AST), coinciding with hepatocellular necrosis. The disease can be caused by medications, such as an overdose of APAP (in the United States), which can be deadly.

1.1.2 Curcumin

Curcumin is the main yellow bioactive component of turmeric (*Curcuma longa* Linn.). It has been shown to possess a wide spectrum of biological actions. These include anti-inflammatory, anti-oxidant, anti-carcinogenic, anti-mutagenic, anti-coagulant, and anti-diabetic activities (4-6). The hepatoprotection of curcumin have been widely acknowledged and used in traditional medicine for treatment of inflammatory conditions such as hepatitis (7). Thus, this study aims to support the use of this active phytochemical as an alternative treatment against toxic liver injury, which may act by preventing the hepatocytes from APAP toxicity. However, it is unclear whether curcumin has any effect in APAP-induced hepatotoxicity.

1.2 Research question

Whether curcumin attenuate hepatitis in mice with paracetamol overdose

1.3 Research objective

To investigate the effects of curcumin could attenuate hepatitis in mice with paracetamol overdose in these parameters:

1. Serum AST and ALT
2. Oxidative stress (MDA)
3. Hepatic GSH
4. Inflammatory cytokines: IL-12 and IL-18
5. Liver histopathology

1.4 Hypothesis

Curcumin attenuate hepatitis in mice with paracetamol overdose.

1.5 Assumption

All animals are not different.

1.6 Key words

APAP; curcumin; oxidative stress; hepatitis; GSH; IL-12; IL-18

1.7 Research design

Animal experimental design

1.8 Expected benefits and application

The findings were relevant in understanding the effects of curcumin attenuate hepatitis in mice with paracetamol overdose and provide a new natural therapeutic agent, curcumin, to protect mice against the development of hepatitis.

CHAPTER II

LITERATURE REVIEWS

2.1 Mechanism of APAP-induced hepatotoxicity

APAP is a widely used analgesic and antipyretic drug (8). APAP toxicity is one of the most widespread drug-induced side-effects worldwide and damage to the liver is a major complication of APAP overdose. APAP metabolites produced in the liver and other organs are likely to be the main contributor into the mechanism of its toxicity (9).

As shown in Figure 2.1, in therapeutic doses, APAP is mainly metabolized via glucuronidation and sulfation and in conjugated forms is excreted from the body. Besides, APAP is partly metabolized by cytochrome P450 (CYP 2E1), to produce some metabolites, mainly N- acetyl-*p*-benzoquinone imine (NAPQI), which are dramatically increased in APAP overdose. These metabolites (NAPQI) are detoxified by reduced glutathione (GSH) and removed from the cells. Then, in APAP overdose causes increasing of toxic metabolites. These metabolites interact with a range of cellular proteins via covalent binding, which disrupting hepatocytes function causing necrosis, apoptosis, and liver injury occurs (10, 11). Currently the standard therapy for APAP-induced toxicity is infusion of N-acetyl cysteine (NAC). NAC is a cysteine pro-drug which works as an anti-oxidant and glutathione precursor.
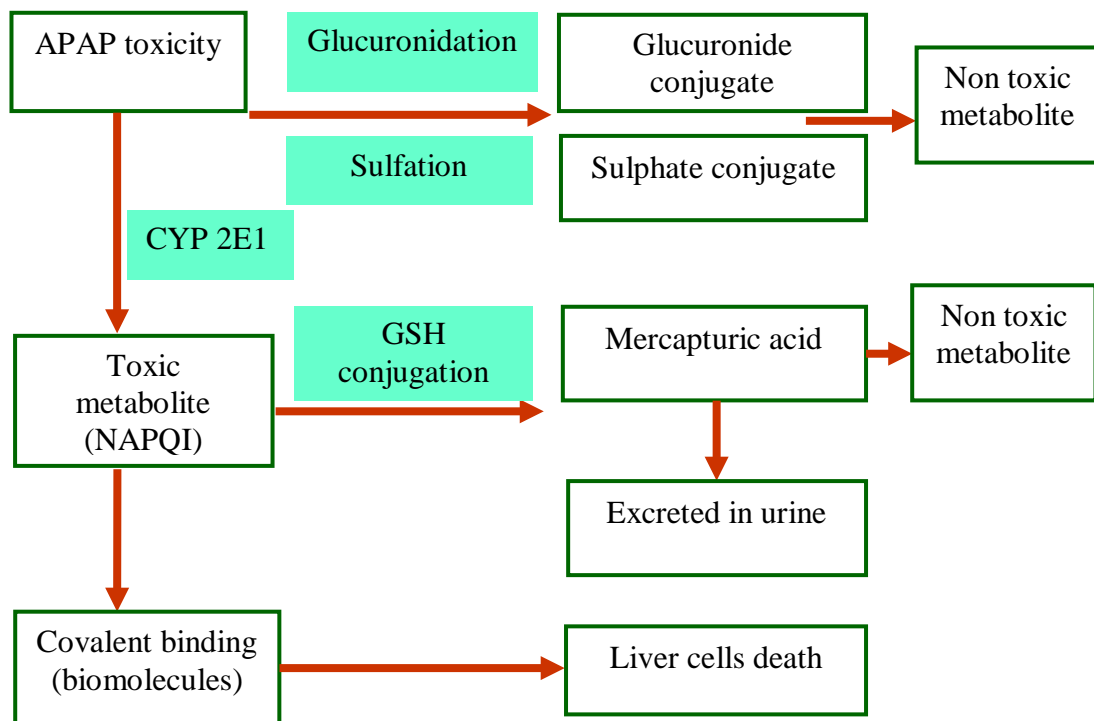
Figure 2.1   Pathway of APAP toxicity on liver cell death

2.2 The liver

The liver is the largest internal organ, weighing approximately 1,500 gram and accounting for nearly 1.5% of adult body weight. It is located in the upper right and partially in the upper left quadrants of the abdominal cavity, protected by the ribcage. The liver is enclosed in a capsule of fibrous connective tissue (Glisson's capsule); a serous covering (visceral peritoneum) surrounds the capsule, except where the liver adheres directly to the diaphragm or the other organs. In human the liver is anatomically divided by deep groves into two lobes (the right and left lobes) and two smaller lobes (the quadrate and caudate).

2.2.1 Structural and functional organization of the liver

The structural and functional organization of the liver has been described by hepatic lobule and hepatic acinus models, respectively. Hepatic lobule is defined histologically as a hexagonal region of hepatocytes which arrange around a central vein. The hepatic acinus is the smallest functional unit that is defined by the terminal branches of the portal triad. Cells in the hepatic acinus can be subdivided into zones (Figure 2.3).

Zone 1 called periportal area would be closest to the vessel and consequently the first to be affected by or to alter the incoming blood. Cell in zone 2 called midzone would be second to respond to the blood and zone 3 called centrilobular or periacinal area would be portal vein blood that has been previously altered by cells in both zone 1 and 2 (12).

Five intrinsic cell types have been identified in the liver: the parenchymal cells or hepatocytes and four types of non-parenchymal cells. The non-parenchymal cells are the liver resident macrophages; the Kupffer cells; endothelial cells; the Stellate cells (also called Ito-or fat storing cells); and the pit cells (12).

2.2.2 Blood supply of the liver

The liver receives blood from two sources, the hepatic artery (25%) with oxygenated blood, and the hepatic portal vein (75%) with deoxygenated blood containing newly absorbed nutrients, drugs, and possibly microbes and toxin from the gastrointestinal tract (13). Branches of both hepatic artery and hepatic portal vein carry blood into liver sinusoids. The blood drains into the central vein. Central veins drain into larger veins often called sublobular veins and these in turn drain into the hepatic veins and empty their blood into the inferior vena cava (Figure 2.4). Branches of the hepatic portal vein, hepatic artery, and bile duct typically accompany each other in their distribution through the liver. Collectively, these three structures are called a portal triad or portal tract (14).

2.2.3 Functions of the liver

The liver performs many vital functions (15) including; first, metabolizing the products of digestion through the portal vein (principally degradation products of protein and carbohydrates); second, the storage and release of substances (principally glucose) so as to maintain a constant level in the blood; and third, the synthesis, conjugation and transformation of substances i.e., formation of protein, detoxification of poisonous substances, production of carbohydrates from protein. All of these are endocrine function which alters the composition of blood traversing the liver.
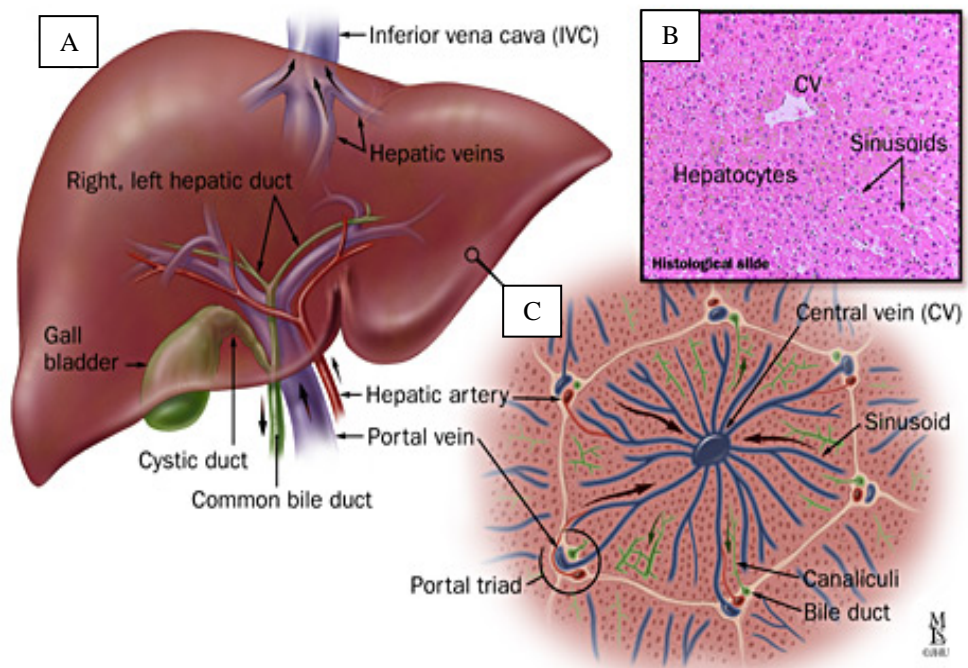
Figure 2.2   Anatomic structure of liver A, normal gross anatomy of liver; B, histological slide; and C, histological view.
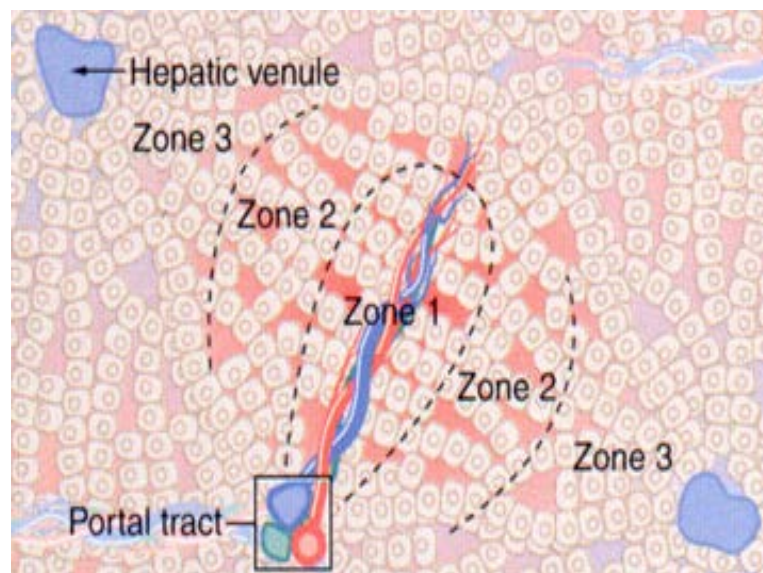
Figure 2.3   The hepatic acinus: the hepatic acinus is divided into zones 1, 2, and 3 and the hepatocytes in these zones have different metabolic functions.
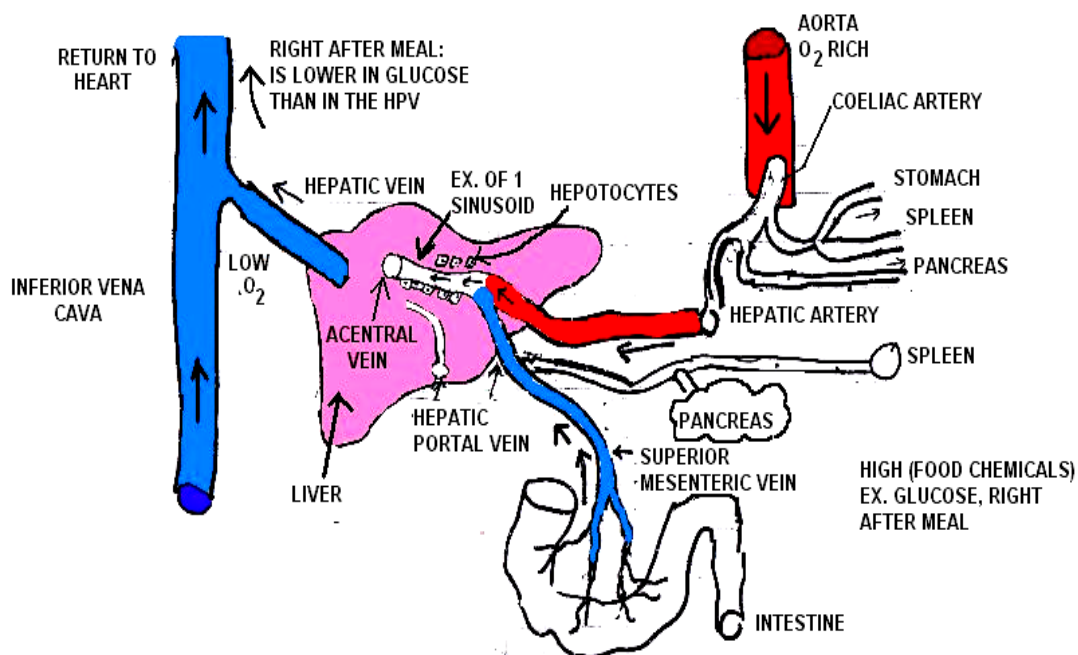
Figure 2.4   Major vessels of the hepatic portal system

2.3 Parameters of hepatotoxicity
2.3.1 Liver Function Tests

Hepatic enzymes, AST and ALT, are found intracellularly in a large number of tissues with highest concentrations in hepatocytes. Hepatic enzymes are often used as markers of liver function (16). There is a significant increase in blood of both AST and ALT in APAP overdose indicates liver damage and deranged integrity of the hepatocytes plasma membrane leaks and/or hepatocytes necrosis. Inflammation of the hepatocytes results in elevation of ALT and AST enzymes.

L-Alanine + Alpha-Ketoglutarate (alpha-KG) $\underline{\text{ALT}}$ L-Glutamate + Pyruvate

Pyruvate + NADH $\underline{\text{Lactate dehydrogenase (LDH)}}$ Lactate + NAD
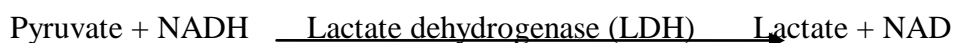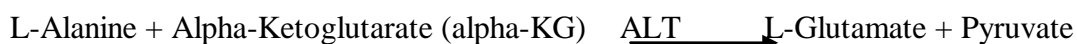
ALT is the enzyme produced within the hepatocytes. The level of ALT abnormality is increased in conditions where hepatocytes have been inflamed or undergone cell death. As the hepatocytes are damaged, the ALT leaks into the bloodstream leading to a rise in the serum levels. Any form of hepatocytes damage can result in an elevation in the ALT. The ALT level may or may not correlate with the degree of cell death or inflammation. ALT is the most sensitive marker for hepatocytes damage.

L-Aspartate + Alpha-KG $\underline{\text{AST}}$ L-Glutamate + Oxaloacetate

Oxaloacetate + NADH $\underline{\text{Malate dehydrogenase (MDH)}}$ Malate + NAD
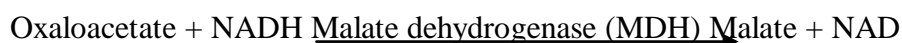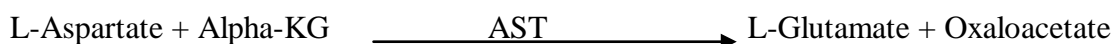
AST enzyme, this enzyme also reflects damage to the hepatocytes. It is less specific for liver disease. It may be elevated and other conditions such as a myocardial infarct. Although AST is not a specific for liver as the ALT, ratios between ALT and AST are useful to physicians in assessing the etiology of liver enzyme abnormalities.

2.3.2. Lipid peroxidation

Lipid peroxidation is a chain reaction process that involves the participation and production of free radical species. Free radicals can cause cellular injury when produced in sufficient amounts to overcome the normally efficient protective mechanism. Lipid peroxidation is a free radical mediated chain reaction which is enhanced as a consequence of oxidative stress (a general term used to describe a stable of damage caused by reactive oxygen species (ROS), and it results in an oxidative deterioration of membrane polyunsaturated fatty acids). It is a continuous physiological process occurring in cell membrane (17), which defined as the oxidative deterioration of polyunsaturated fats. The rate of oxidation of fatty acids increases with the degree of unsaturation. The membrane of mammalian cells contains large amount of polyunsaturated fatty acids which are especially susceptible to lipid peroxidation. Lipid peroxidation of cell membrane results in decreased membrane fluidity, inability to maintain ionic gradients, cellular swelling, and tissue inflammation. It involved the reaction of oxygen and polyunsaturated lipids to form lipid free radicals and hydroperoxides, which in turn promote free radicals chain reaction as show in Figure 2.5.
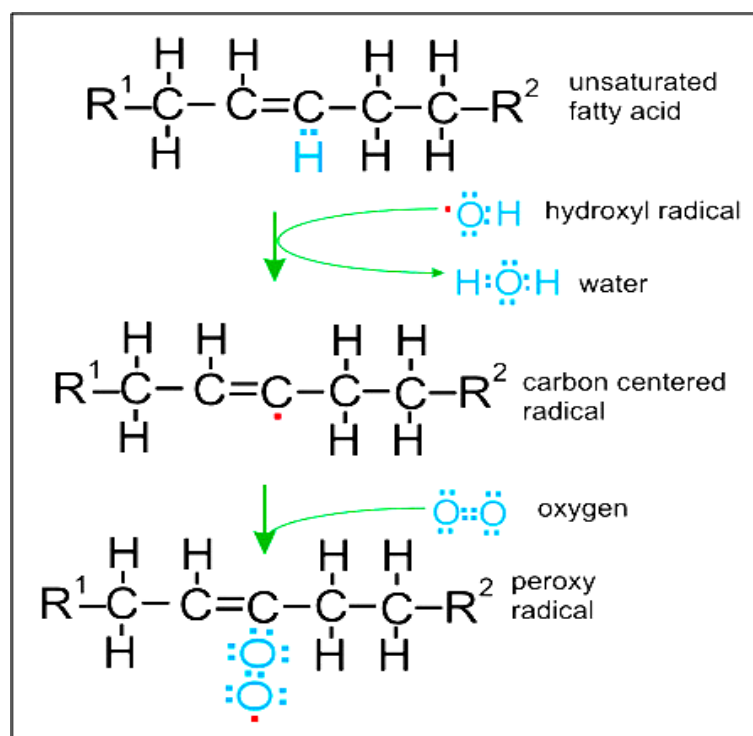
Figure 2.5   Illustration of lipid peroxidation

Thiobarbituric acid (TBA) is the most widely used test for measuring the extent of lipid peroxidation in foods due to its simplicity and because its results are highly correlated with sensory evaluation scores. The basic principle of the method is the reaction of one molecule of malondialdehyde (MDA) and two molecules of TBA to form a red MDA-TBA complex, which can be quantitated spectrophotometrically at 532 nanometer (nm). However, this method has been criticized as being nonspecific and insensitive for the detection of low levels of MDA. Other thiobarbituric acid reactive substances (TBARs) including sugars and other aldehydes could interfere with the MDA-TBA reaction. Abnormally low values may result if some of the MDA reacts with proteins in an oxidizing system. In many case, however, the TBA test is applicable for comparing samples of a single material at different states of oxidation.

2.3.3 Interleukin (IL)-12

IL-12, also known as natural killer cells stimulatory factor (NKSF) or cytotoxic lymphocyte maturation factor (CLMF), is a pleiotropic cytokine originally identified in the medium of a human B-lymphoblastoid cell line (18-20). IL-12 has been shown to have multiple effects on T lymphocytes and natural killer (NK) cells. Some of these effects include the induction of interferon-gamma (IFN-γ) and tumor necrosis factor (TNF) production by T and NK cells, the enhancement of cytotoxic activity of T and NK cells and the stimulation of T and NK cell proliferation. IL-12 has also been shown to be a central mediator of the cell-mediated immune response by promoting T helper type 1 (Th1) development (21-25).

2.3.4 Interleukin (IL)-18

IL-18 is an 18 kilodalton novel cytokine which is identified as a co-stimulatory factor for production of IFN-γ in response to toxic shock. It shares functional similarities with IL-12. IL-18 is synthesized as a precursor 24 kilodalton molecule without a signal peptide and must be cleaved to produce an active molecule. IL-1 converting enzyme (ICE, Caspase-1) cleaves pro-IL-18 at aspartic acid in the P1 position, producing the mature, bioactive peptide that is readily released from cells. It has been reported that IL-18 is produced by Kupffer cells, activated macrophages, keratinocytes, intestinal epithelial cells, osteoblasts, adrenal cortex cells, and murine diencephalon. IFN-γ is produced by activated T and NK cells and plays critical roles in the defense against microbial pathogens. IFN-γ activates macrophages, enhances NK activity and B cell maturation, proliferation and Ig secretion, induces MHC class I and II antigens expression, and inhibits osteoclast activation. IL-18 acts on Th1 cells and in combination with IL-12 is strongly induced production of IFN-γ by these cells. Pleiotropic effects of IL-18 have also been reported, including enhancement production of IFN-γ and GM-CSF in peripheral blood mononuclear cells, production of Th1 cytokines, IL-2, GM-CSF and IFN-γ in T cells, and enhancement of Fas ligand expression by Th1 cells (26-30).
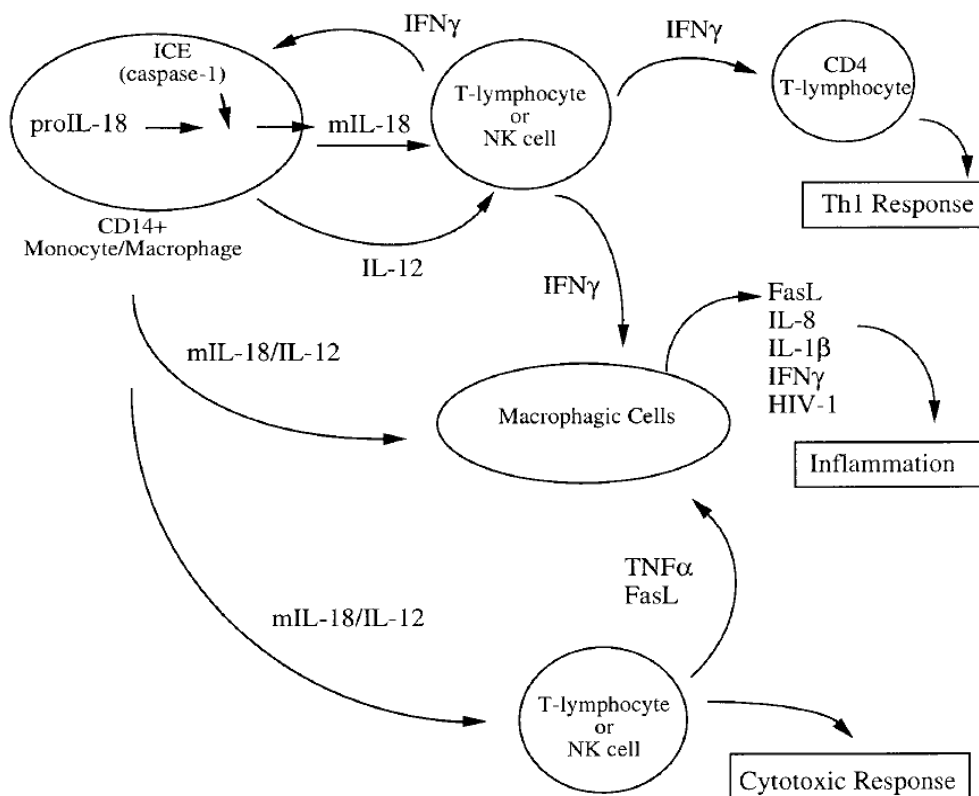
Figure 2.6   Pathways of IL-12 and IL-18 in the inflammation response (31)

2.4 Parameter of hepatoprotection

GSH: GSH is a tripeptide (γ-glutamylcysteinylglycine) that widely distributed in both plant and animal (32, 33). GSH serves a nucleophilic co-substrate to glutathione transferase in the detoxification of xenobiotics and is an essential electron donor to glutathione peroxidases in the reduction of hydroperoxides (33, 34). GSH is also involved in amino acid transport and maintenance of protein sulfhydryl reduction status (35, 36). Concentration of GSH ranges from a few micromolar (μM) in plasma to several millimolar (mM) in tissues, such as liver (37, 38).
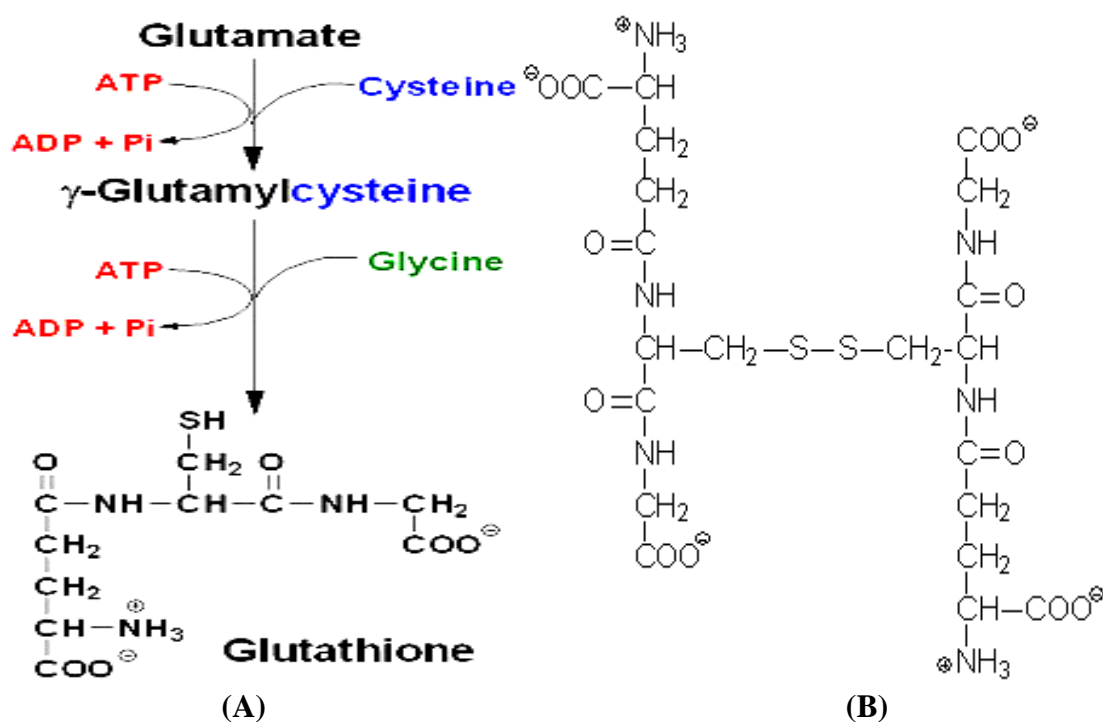
Figure 2.7   Schematic of glutathione synthesis and metabolism; (A) reduced form (GSH) and (B) oxidized form (GSSG)

2.5 Curcumim

Curcumin is the main yellow bioactive component of turmeric (*Curcuma longa* Linn.). It has been shown to possess a wide spectrum of biological actions. These include anti-inflammatory, anti-oxidant, anti-carcinogenic, anti-mutagenic, anti-coagulant, and anti-diabetic activities (7-9). The hepatoprotection of curcumin have been widely acknowledged and used in traditional medicine for treatment of inflammatory conditions such as hepatitis (10). The structure of curcumin is depicted in Figure 2.9.

Figure 2.8   *Curcuma longa* Linn.
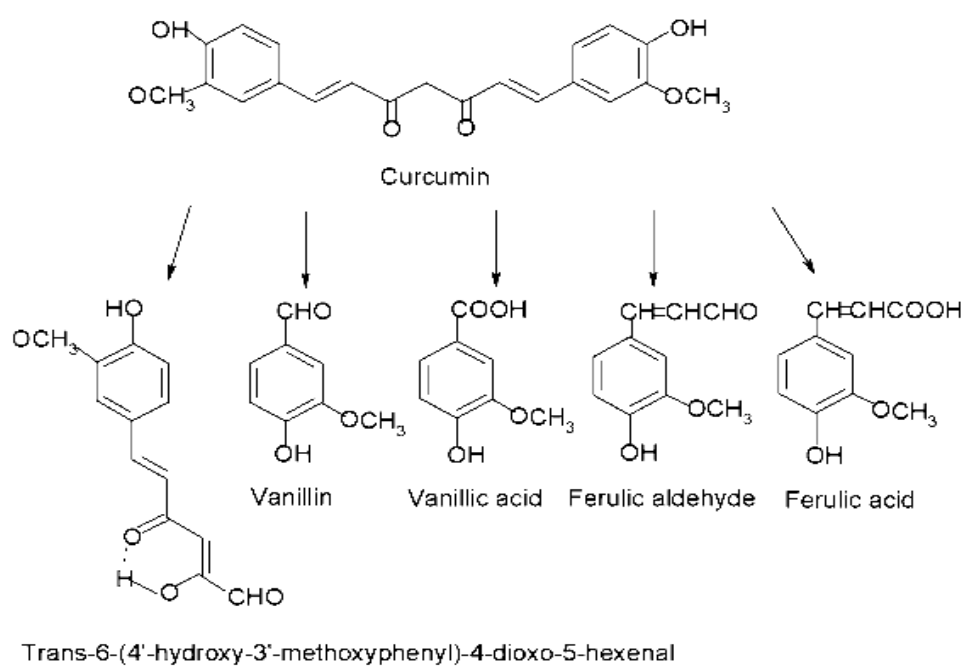
Figure 2.9   Chemical structures of curcumin (*diferuloylmethane*) and its decomposition products (39)
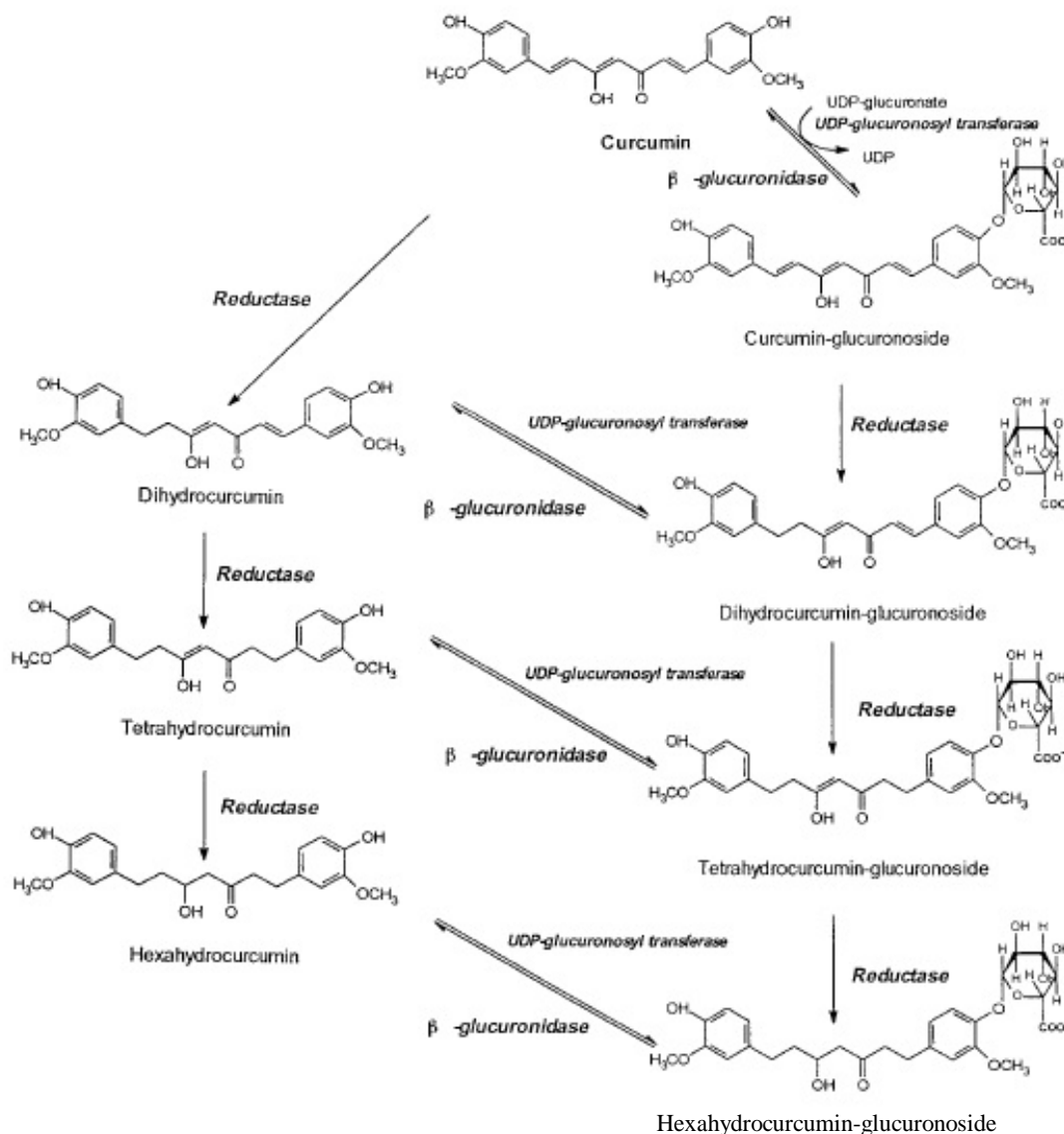
Figure 2.10   Proposed biotransformation and metabolites of curcumin in mice plasma (40).

Pharmacokinetic Study and Safety

Curcumin is dissolved in organic solvents such as dimethylsulfoxide, oil, alcohol, and petroleum agents. In animals, the previous study demonstrated that curcumin is poorly absorbed and rapidly metabolized in Sprague-Dawley rats (41-44). Administrating curcumin orally was made by Wahlstrom B and Blennow G (41). They demonstrated that this compound in a dose of 1 to 5 gram per kilogram (g/kg) body weight (BW) given to rats apparently did not cause any adverse effects and it was excreted about 75% in the feces, while traces appeared in the urine. In addition, measurements of blood plasma levels and biliary excretion showed that curcumin was poorly absorbed by the gastrointestinal tract.

In 1999, Pan MH et al. investigated the pharmacokinetic properties of curcumin in mice. After intraperitoneal administration of curcumin (0.1 g/kg) in mice,

approximately 2.25 microgram per millilitre (μg/mL) of curcumin appeared in the plasma within the first 15 minute. To clarify the nature of the metabolites of curcumin, the plasma was analyzed by reversed-phase HPLC and two putative conjugates of curcumin were observed. To investigate the nature of these glucuronide conjugates *in vivo*, the plasma was analyzed by electrospray. Curcumin was first biotransformed to dihydrocurcumin and tetrahydrocurcumin, and that these compounds subsequently were converted to monoglucuronide conjugates. Ireson C et al. studied the biotransformation of curcumin by human and rat hepatocytes and identified hexahydrocurcumin and hexahydrocurcuminol as the major metabolites of curcumin (45).

Curcumin has been demonstrated that safety in human and rats. Oral LD_{50} of curcumin was found to be 12.2 g/kg BW in rats (46). Human appeared to be able to tolerate high doses of curcumin without significant side-effects. A phase 1 study by Cheng AL et al. (47), found no adverse effects of curcumin ingestion for 3 months of doses up to 8,000 milligram per day (mg/day).

Antioxidant Property of Curcumin

The discovery of the antioxidant properties of curcumin explains many of its wide ranging pharmacological activities. The phenolic and methoxy groups on the benzene rings are important structural features that contribute to its antioxidant properties (48, 49). Curcumin is an effective antioxidant and scavenges superoxide radical (O_2^-), hydrogen peroxide (H_2O_2) radical, and nitric oxide from activated macrophages (50). It inhibited the inducible nitric oxide synthase (iNOS) activity in macrophages (51). Oral administration of 30 mg/kg BW of curcumin in rats for 10 days reduced the iron-induced hepatic damage by lowering lipid peroxidation (52). Protection from radiation by dietary curcumin administered to mice is also attributed to the antioxidant property of curcumin. In addition, curcumin inhibited liver injury in carbon tetrachloride (CCl_4) induced hepatotoxicity in rats (53). Interestingly, curcumin enhanced the activities of other antioxidants, such as superoxide dismutase (SOD), catalase, and glutathione peroxidase (54).

Anti-inflammatory Property of Curcumin

Macrophages, when activated, generate a number of proinflammatory cytokines. The pleiotropic cytokine, TNF-α, induces the production of IL-1β, and together, they play significant roles in many acute and chronic inflammatory and autoimmune diseases. *In vitro* studies show that curcumin, at 5μM, inhibited the lipopolysaccharide (LPS)-induced production of TNF-α and IL-1β by a human monocytic macrophage cell line (55, 56). As a consequence, downstream events involving TNF-α and IL-1β are affected. All these studies showed that curcumin is an anti-inflammatory substance because it can inhibit the activation of the major inflammatory cytokines. These cytokines required for the expression of many cells linked with immune response, such as TNF-α, IL-1β, iNOS, and COX-2

2.6 The hepatoprotection of curcumin on APAP-induced hepatotoxicity

2.6.1 The hepatoprotection of curcumin on APAP-induced GSH depletion and liver inflammation

APAP toxicity occurred with activation of Kupffer cells (hepatic macrophages) indicated that Kupffer cell activation led to increase in pro-

inflammatory cytokines. Cytokines have important functions in immunity, inflammation, cell proliferation, differentiation, and cell death (57).

Curcumin modulated the inflammatory response by down-regulating the activity of cyclooxygenase-2 (COX-2), lipoxygenase, and iNOS enzymes, inhibiting the production of the inflammatory cytokines, TNF-α, IL-1, IL-2, IL-6, and IL-8 (58). Curcumin was also found to be a potent inhibitor of rat liver (CYP 1A1/1A2), a less potent inhibitor of (CYP 2B1/2B2), and a weak inhibitor of (CYP 2E) (59). Hepatic GSH was significantly decreased due to APAP overdose. Girish C et al. (60) showed that treatment of mice with a single dose of 50 milligram per kilogram (mg/kg) and 100 mg/kg of curcumin by oral gavage prior to APAP administration (500 mg/kg, oral gavage) significantly increased hepatic GSH.

2.6.2 The hepatoprotection of curcumin on APAP-induced oxidative stress and liver injury

Girish C et al. (60) showed that treatment of mice with a single dose of 500 mg/kg of APAP showed significantly increased in serum ALT and AST enzymes and hepatic MDA. Histological examination showed a severe centrilobular hepatic necrosis with fatty changes in the lobule. Pre-treatment of mice with a single dose of 50 mg/kg and 100 mg/kg of curcumin significantly decreased these parameters toward normal values and the improvement of liver histopathology.

Kheradpezhouh E et al. (61) showed that treatment of rats with a single dose of 700 mg/kg of APAP by intraperitoneal (i.p.) injection showed significantly elevated serum ALT and AST enzymes and hepatic MDA. The histological examination showed a severe centrilobular hepatic necrosis in the lobule. Post-treatment of rats with 25, 50, and 100 mg/kg of curcumin by i.p. injection after APAP administration significantly decreased the hepatic MDA, hepatic enzymes, and the improvement of liver histopathology in a dose-dependent manner.

Yousef MI et al. (62) showed that treatment of rats with a single dose of 650 mg/kg of APAP by oral gavage showed significantly elevated in hepatic MDA. These were associated with evidence of hepatic necrosis and elevated serum ALT and AST enzymes. Post-treatment of rats with a single dose of 50 mg/kg of curcumin by oral gavage after APAP administration significantly decreased the hepatic MDA, hepatic enzymes, and the improvement of liver histopathology. Therefore, curcumin can protect the liver from the damage caused by APAP overdose.

CHAPTER III

MATERIALS AND METHODS

3.1 Materials

Male mice (4-5 weeks of age), weighing 25-30 gram, were purchased from the National Laboratory Animal Center, Mahidol University (Bangkok, Thailand). A single dose of 400 mg/kg of APAP also known as Tylenol®was administered to mice by oral gavage. Curcumin was purchased from Cayman Chemical Company (Ann Arbor, MI, USA). A single dose of 200 and 600 mg/kg of curcumin were administered to mice by oral gavage. The experimental protocol was approved by the Ethical Committee of Faculty of Medicine, Chulalongkorn University, Thailand. The mice were acclimatized at least 1 week in a climate-controlled room on a 12-hour light-dark cycle and were fed *ad libitum*.

MDA reagents and equipments
- 1.15% Potassium chloride (KCI) buffer
- 20% Acetic acid
- 0.8% TBA
- 8.1% Sodium dodecyl sulfate (SDS)
- 1,1,3,3 Tetramethoxypropane (TMP)
- 37% Hydrochloric acid (37% HCl)
- 1N Sodium hydroxide (1N NaOH)
- Distilled water
- Waterbath
- Repeat pipettor
- Spectrophotometer

GSH reagents and equipments (Cayman Chemical Company, USA)
- GSH MES Buffer (2X)
- GSSG Standard
- GSH Co-Factor Mixture
- GSH Enzyme Mixture
- GSH DTNB
- A source of pure water; glass distilled water or HPLC–grade water
- Metaphosphoric acid and triethanolamine
- Phosphate buffer saline (PBS)
- Orbital shaker
- An adjustable pipettor, repeat pipettor, and eight channel pipettor
- 96-Well Plate (Colorimetric Assay)
- 96-Well Plate Covers
- Microplate reader

IL-12 reagents and equipments (R&D Systems, Inc., USA)
- Mouse IL-12 p70 Conjugate (23 millilitre (mL)/vial of a polyclonal antibody against mouse IL-12 p70 conjugated to horseradish peroxidase)

- Mouse IL-12 p70 Standard (2.5 nanogram (ng)/vial of recombinant mouse IL-12 p70 in a buffered protein base; lyophilized)
- Mouse IL-12 p70 Control (Recombinant mouse IL-12 p70 in a buffered protein base; lyophilized)
- Assay Diluent RD1-14 (12.5 mL/vial of a buffered protein solution)
- Calibrator Diluent RD5Y (21 mL/vial of a buffered protein solution)
- Wash Buffer Concentrate (50 mL/vial of a 25-fold concentrated solution of a buffered surfactant)
- Color Reagent A (12.5 mL/vial of stabilized hydrogen peroxide
- Color Reagent B (12.5 mL/vial of stabilized chromogen; tetramethylbenzidine)
- Stop Solution (23 mL/vial of a diluted hydrochloric acid solution)
- Deionized or distilled water
- Mouse IL-12 p70 Microplates
- Pipettes and pipette tips
- Squirt bottle, manifold dispenser, or automated microplate washer
- 100 mL and 1000 mL graduated cylinders
- Polypropylene tubes
- Plate covers (adhesive strips)
- Microplate reader

IL-18 reagents and equipments (Medical & Biological Laboratory Co., Ltd, Japan)
- Mouse IL-18 Calibrator (Lyophilized)
- Conjugate Reagent (X101) (Peroxidase conjugate anti-mouse IL-18 monoclonal antibody)
- Conjugate Diluent
- Assay Diluent
- Wash Concentrate (10X)
- Substrate (Tetramethylbenzidine/Hydrogen Peroxide)
- Stop Solution (0.5 molar (M) H_2SO_4)
- distilled water
- Microwell Strips coated with anti-Mouse IL-18 antibody (8 well strips)
- Plate washer or washing bottle
- Adjustable micropipette
- Multichannel micropipette
- 96-well polyvinyl plate
- Microplate holder
- Uncoated microwell strips
- Reagent vessel
- Plate Covers
- Microplate reader

3.2 Experimental Protocols

The mice were then fasted for 16 hour before experiments to sensitize mice to APAP toxicity. APAP was dissolved in distilled water while curcumin in powder form was dissolved in corn oil that was freshly prepared for the experiment. Male mice were randomly divided into four groups.

Group I (Control group); mice were gavaged with distilled water.

Group II (APAP group); mice were gavaged with a single dose of 400 mg/kg of APAP.

Group III (APAP + CUR 200 group); mice were gavaged with a single dose of 400 mg/kg of APAP with a single dose of 200 mg/kg of curcumin.

Group IV (APAP + CUR 600 group); mice were gavaged with a single dose of 400 mg/kg of APAP with a single dose of 600 mg/kg of curcumin.

```
                    ┌─────────────────────────────┐
                    │  Male mice 25-30 g (n = 32)  │
                    └─────────────────────────────┘
```

| Control group: distilled water, n = 8 | APAP group: APAP single dose 400 mg/kg, n = 8 | APAP + CUR 200 group: APAP single dose 400 mg/kg + curcumin single dose 200 mg/kg, n = 8 | APAP + CUR 600 group: APAP single dose 400 mg/kg + curcumin single dose 600 mg/kg, n = 8 |

```
                          24 hours
```

The parameters were measured in this study.
- GSH level in liver
- MDA level in liver
- IL-12 level in serum
- IL-18 level in serum
- AST and ALT levels in serum
- Liver histopathology

Twenty-four hour after distilled water administration in the first group, APAP administration in the second group, and APAP with CUR administration in the other two groups, the mice were anesthetized with i.p. injection of thiopental sodium (50 mg/kg body weight). The abdomen was opened medially and the whole liver was rapidly removed and washed with cold normal saline (4-8°C). The tissues were chopped into small pieces with scissors, frozen in liquid nitrogen, and stored at -80°C for lipid peroxidation (hepatic MDA) and hepatic GSH assays by glutathione assay kit. The remaining liver was fixed in 10% formalin solution for histological examination. Subsequently, the whole blood of mice was withdrawn directly from the heart. The blood was allowed to coagulate at room temperature (2 hours) and the samples were then centrifuged for 20 minutes at 3000 revolution per minute (r.p.m.) to obtain serum. The serum sample was collected for the hepatic enzymes (AST and ALT) and inflammatory cytokines (IL-12 and IL-18) assays by mouse IL-12 p70 immunoassay and mouse IL-18 enzyme-linked immunosorbent assay (ELISA) kit, respectively.

3.3 Methods

3.3.1 Serum aiminotransferase (AST and ALT) assays

Principle of the assay: AST transfer an amino group from aspartate to alpha-KG and produce oxaloacetate and glutamate. ALT transfers an amino group from alanine to alpha-KG and produce pyruvate and glutamate. The products, oxaloacetate and pyruvate, form complex with 2, 4 dinitrophenyl hydrazine (2, 4 DNPH) and a red colored is produced on the addition of sodium hydroxide (Figure 3.1).

R, R' = hydrogen or alkyl

2, 4 DNPH   2, 4 dinitrophenyl hydrazone (red colored)
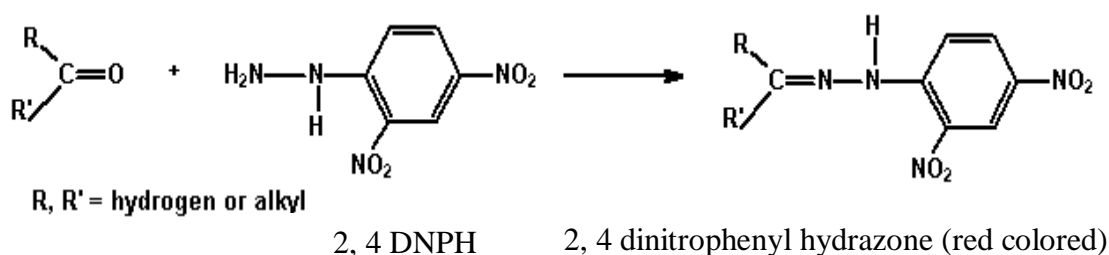
Figure 3.1   Complex of products, oxaloacetate or pyruvate, with 2, 4 DNPH

3.3.2 Hepatic MDA assay

Principle of the assay: MDA, a product of lipid peroxidation, forms a 1:2 adduct with TBA in acidic condition and at 90°C. The TBA-MDA complex (pink-colored) is measured by spectrophotomer at 532 nm (63) (Figure 3.2).
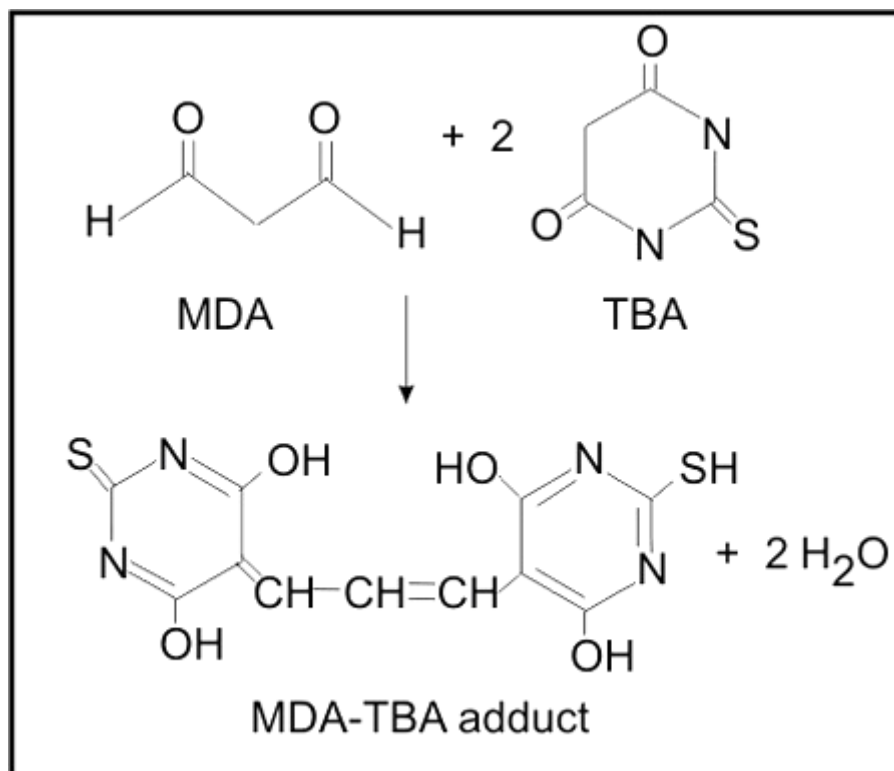
Figure 3.2   Reaction of MDA with TBA

Procedure: Reagent preparation
- 8.1% SDS: Add 8.1 gram of 8.1% SDS into the 100 mL of distilled water. Do not shake and store at 4°C.
- 20% acetic acid: Pipette 26.61 mL of 37% HCl into the 973.49 mL of distilled water. Add 20 mL of pure acetic acid into the 80 mL of HCl. Adjust pH (3.5) of the reagent with 1N NaOH.
- 0.8% TBA: Add 0.8 gram of TBA into the 100 mL of distilled water, heat, and stirrer until the crystals have completely dissolved.
- TMP (Standard): Pipette 16.4 microlitre (μL) of TMP into the 100 mL of distilled water (stock TMP) and pipette 0.04, 0.08, 0.12, 0.16, and 0.20 μL of stock TMP into the 10 mL of distilled water.

Assay procedure
Lipid peroxidation of mice liver using TBA was measured by a modified method of Ohkawa H et al. (64).
- One gram of the liver was homogenized in 1.15% KCl buffer on ice.
- An aliquot of 0.2 mL was mixed with solution containing 20% acetic acid, 0.8% TBA, and 8.1% SDS, heated in waterbath at 95°C for 60 minutes and then cooling with tap water for 30 minutes at room temperature. Add 1 mL of distilled water and 0.5 mL of mixture of n-butanol and pyridine and shake vigorously at least 1 minute.

- The solution was centrifuged for 15 minutes at 3500 r.p.m. and the absorbance of the supernatant fraction was determined at a wavelength of 532 nm. 1,1,3,3 TMP was used as a standard of MDA.

- The MDA content was calculated in comparison with a standard MDA curve and was expressed in terms of nanomole per milligram (nmol/mg) protein (Figure 3.3).

Figure 3.3   Example of standard MDA curve: plot of corrected absorbance at 532 nm versus MDA concentration

$$[MDA] = \frac{[(Absorbance\ at\ 532\ nm) - (Y\text{-}intercept)] \times Dilution\ factor}{Slope}$$

* If samples have been diluted, the concentration read from the standard curve must be multiplied by the dilution factor.

3.3.3 Hepatic GSH assay

Hepatic GSH was determined using a commercially available GSH Assay Kit (Cayman Chemical Company, USA).

Principle of the assay: Cayman' GSH Assay utilizes a carefully optimized enzymatic recycling method, using glutathione reductase, for the quantification of GSH (65-67) (Figure 3.4). The sulfhydryl group of GSH reacts with 5, 5'-dithio-*bis*-(2-nitrobenzoic acid) (DTNB), or Ellman's reagent and produces a yellow colored 5-thio-2-nitrobenzoic acid (TNB). The mixed disulfide, GSTNB (between GSH and TNB) that is concomitantly produced, is reduced by glutathione reductase to recycle the GSH and produce more TNB. The rate of TNB production is directly proportional to this recycling reaction which is in turn directly proportional to the concentration of GSH in the sample. Measurement of the optical density (O.D.) of TNB at 405-414 nm provides an accurate estimation of GSH in the sample.

GSSG

GR

TNB ← ← GSH ← DTNB

GR

GSTNB ← ← TNB
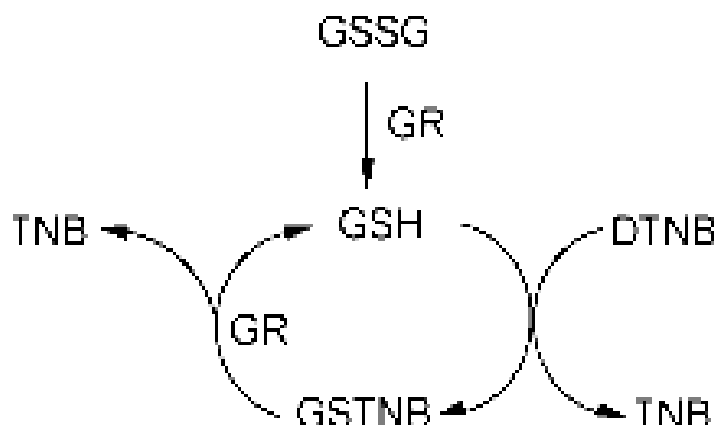
Figure 3.4   GSH recycling

GSH is easily oxidized to the disulfide dimer (oxidized glutathione; GSSG). GSSG is produced during the reduction of hydroperoxides by glutathione peroxidase. GSSG is reduced to GSH by glutathione reductase and it is the reduced form that exists mainly in biological systems. However, samples will require deproteination.

Procedure: Reagent preparation

- GSH MES buffer (2X): The buffer consists of 0.4 M 2-(N-morpholino) ethanesulphonic acid, 0.1 M phosphate, and 2 mM EDTA, pH 6.0. Dilute 60 mL of the buffer with 60 mL of HPLC-grade water before use. Hereafter, MES buffer refers to this diluted buffer.

- GSSG standard: Each vial contains 2 mL of 25 µM GSSG in MES buffer. This standard is ready to use as supplied. The standard is stable for at least one year if stored as supplied at 0-4°C.

- GSH co-factor mixture: The vials contain a lyophilized powder of NADP^{+} and glucose-6-phosphate. Reconstitute the contents of the vial with 0.5 mL of water and mix well. This is enough co-factor mixture for 96 wells. The reconstituted reagent will be stable for two weeks if stored at 0-4°C.

- GSH enzyme mixture: The vials contain glutathione reductase and glucose-6-phosphate dehydrogenase in 0.2 mL buffer. Add 2 mL of diluted MES buffer to the vial, replace the cap, and mix well. This is enough enzyme mixture for 96 wells. The reconstituted enzyme mixture will be stable for two weeks if stored at 0-4°C.

- GSH DTNB: Each vial contains a lyophilized powder of DTNB. Reconstitute the contents of the vial with 0.5 mL of water and mix well. The reconstituted reagent must be used within 10 minutes. Reconstitution of this reagent should be just prior to its addition to the assay cocktail.

Tissue homogenate

- Prior to dissection, either perfuse or rinse tissue with a PBS solution, pH 7.4, to remove any red blood cells and clots.

- Homogenize the tissue in 5-10 mL of cold buffer (i.e., 50 mM MES or phosphate, pH 6-7, containing 1 mM EDTA) per gram tissue.

- Centrifuge at 10000 g for 15 minutes at 40°C.

- Remove the supernatant and store on ice.

- The supernatant will have to be deproteinated before assaying. The sample will be stable for at least six months.

Standard preparation

- Take eight clean test tubes and mark them A-H. Aliquot the GSSG standard (Item No. 703014) and MES buffer to each tube as described in Table 3.1

Tube	GSSG standard (µL)	MES buffer (µL)	Final concentration (µM GSSG)	Equivalent total GSH (µM)
A	0	500	0	0
B	5	495	0.25	0.5
C	10	490	0.5	1.0
D	20	480	1.0	2.0
E	40	460	2.0	4.0
F	80	420	4.0	8.0
G	120	380	6.0	12.0
H	160	340	8.0	16.0

Table 3.1   GSH standards

Assay procedure

- Add 50 µL of standard (tubes A-H) per well in the designated well on the plate.

- Add 50 µL of sample to each of the sample wells.

- Cover the plate with the plate cover provided.

- Prepare the assay cocktail by mixing the following reagents in a 20 mL vial: MES buffer (11.25 mL), reconstituted co-factor mixture (0.45 mL), reconstituted enzyme mixture (2.1 mL), water (2.3 mL), and reconstituted DTNB (0.45 mL). The volumes of reagents given are for the use of the entire plate. Prepare fresh assay cocktail and run a standard curve each time the assay is performed. Use the assay cocktail within 10 minutes of preparation.

- Remove the plate cover and add 150 µL of the freshly prepared assay cocktail to each of the wells containing standards and samples using a multichannel pipette. Replace the plate cover and incubate the plate in the dark on an orbital shaker.

- Determine the O.D. of each well, using a microplate reader set to 405-414 nm at five minutes intervals for 30 minutes (a total of 6 measurements).

Calculation of results

GSH concentration of the samples can be determined by

- Calculate the average absorbance from the 30 minutes measurement for each standard and sample.

- Subtract the absorbance value of the standard A from itself and all other values (both standards and samples). This is the corrected absorbance.

- Plot the corrected absorbance values of each standard as a function of the concentration of GSH of Table 3.1 and Figure 3.5.

- Calculate the values of GSH for each sample from the standard curve.
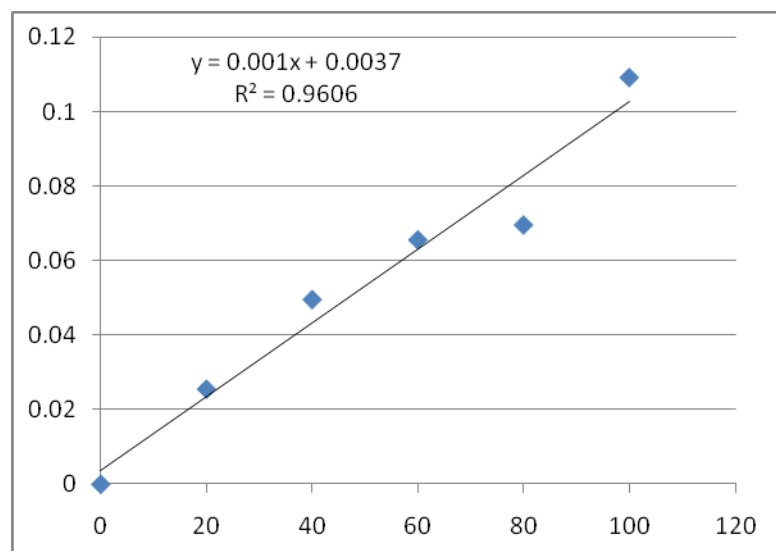

Figure 3.5   Example of standard GSH curve: plot of corrected absorbance at 405 nm versus GSH concentration

$$[\text{GSH}] = \frac{[(\text{Absorbance at 405-414 nm}) - (\text{Y-intercept})] \times 2^* \times \text{Dilution factor}}{\text{Slope}}$$

* If sample required deproteination, multiply by "2" to account for the addition of MPA reagent. If samples have been diluted, the concentration read from the standard curve must be multiplied by the dilution factor.

3.3.4 Serum IL-12 assay

Serum IL-12 was determined using a commercially available mouse IL-12 p70 Kit (R&D Systems, Inc., USA).

Principle of the assay: This assay employs the quantitative sandwich enzyme immunoassay technique. A monoclonal antibody specific for mouse IL-12 p70 has been pre-coated onto a microplate. Standards, controls, and samples are pipette into the wells and any mouse IL-12 p70 present is bound by the immobilized antibody. After washing away any unbound substances, an enzyme-linked polyclonal antibody specific for mouse IL-12 p70 is added to the wells. Following a wash to remove any unbound antibody-enzyme reagent, a substrate solution is added to the wells. The enzyme reaction yields a blue product that turns yellow when the stop solution is added. The intensity of the color measured is in proportion to the amount of mouse IL-12 p70 bound in the initial step. The sample values are then read off the standard curve.

Procedure: Reagent preparation

- Bring all reagents to room temperature before use.

- Mouse IL-12 p70 kit control: Reconstitute the kit control with 1.0 mL deionized or distilled water. Assay the control undiluted.

- Wash buffer: If crystals have formed in the concentrate, warm to room temperature and mix gently until the crystals have completely dissolved. To prepare enough wash buffer solution for one plate, add 25 mL wash buffer concentrate into deionized or distilled water to prepare 625 mL of wash buffer.

- Substrate solution: Color reagent A and B should be mixed together in equal volumes within 15 minutes of use and protect from light. 100 µL of the resultant mixture is required pet well.

- Mouse IL-12 p70 standard: Reconstitute the mouse IL-12 p70 standard with 5.0 mL of calibrator diluent RD5Y. Do not substitute other diluents. This reconstitution produces a stock solution of 500 picograms per millilitre (pg/mL). Allow the standard to sit for a minimum of 5 minutes with gentle mixing prior to making dilutions.

- Pipette 200 µL of calibrator diluent RD5Y into each tube (use polypropylene tubes). Use the stock solution to produce a dilution series (Figure 3.6). Mix each tube thoroughly before the next transfer. Use the undiluted mouse IL-12 p70 standard as the high standard (500 pg/mL) and calibrator diluent RD5Y as the zero standard (0 pg/mL).
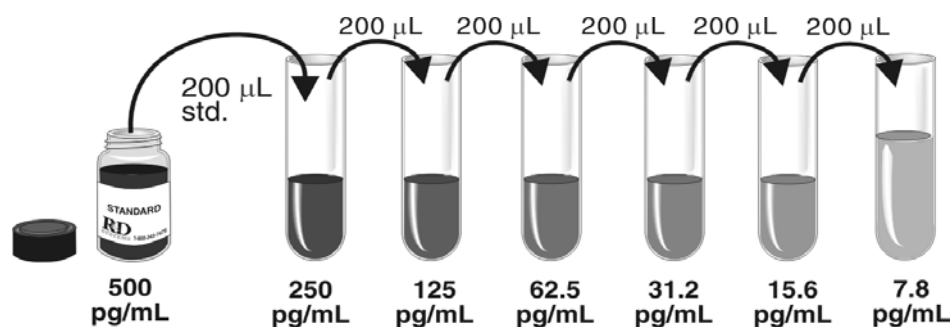
Figure 3.6   Use the stock solution to produce a dilution series

Assay procedure

- Bring all reagents and samples to room temperature before use. It is recommended that all samples, standards, and control be assayed in duplicate.

- Prepare all reagents, working standards, and samples as directed in the previous sections.

- Add 50 µL of assay diluent RD1-14 to each well. Assay diluent RD1-14 may contain undissolved material even when mixed well before and during use.

- Add 50 µL of standard, control, or sample per well. Mix by gently tapping the plate frame for 1 minute. Cover with the adhesive strip provided. Incubate for 2 hour at room temperature. Plate layouts are provided to record standards and samples assayed.

- Aspirate each well and wash, repeating the process four times for a total of five washes. Wash by filling each well with wash buffer (400 µL) using a squirt bottle. Complete removal of liquid at each step is essential to good performance. After the last wash, remove any remaining wash buffer by aspirating or decanting. Invert the plate and blot it against clean paper towels.

- Add 100 µL of Mouse IL-12 p70 conjugate to each well. Cover with a new adhesive strip. Incubate for 2 hours at room temperature.

- Repeat the aspiration/wash

- Add 100 µL of substrate solution to each well. Incubate for 30 minutes at room temperature. Protect from light.

- Add 100 mL of stop solution to each well. Gently tap the plate to ensure thorough mixing.

- Determine the O.D. of each well within 30 minutes, using a microplate reader set to 450 nm.

Calculation of results

- Average the duplicate readings for each standard, control, and sample and subtract the average zero standard optical density.

- Construct a standard curve by plotting the mean absorbance for each standard on the y-axis against the concentration on the x-axis and draw a best fit curve through the points on the graph. The data may be linearized by plotting the log of the mouse IL-12 p70 concentrations versus the log of the O.D. and the best fit line can be determined by regression analysis. If samples have been diluted, the concentration read from the standard curve must be multiplied by the dilution factor (Figure 3.7).
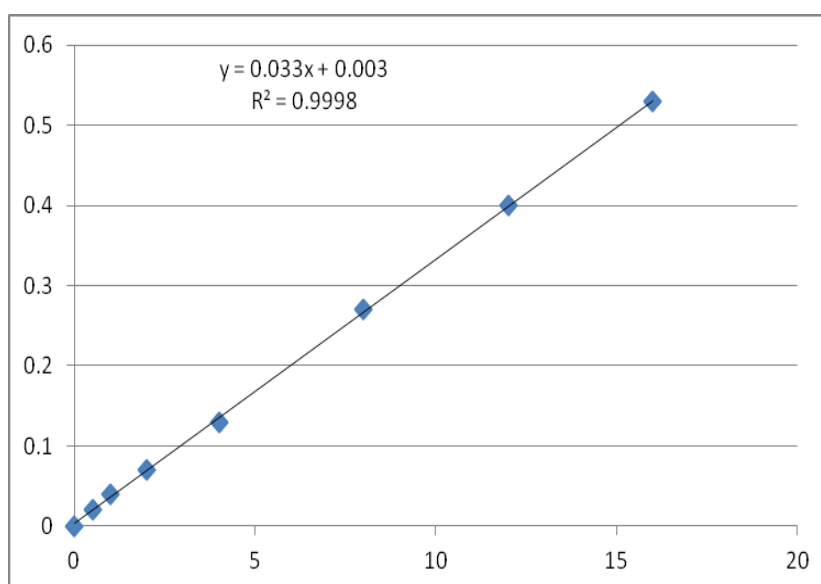
Figure 3.7   Example of standard IL-12 curve: plot of corrected absorbance at 450 nm versus mIL-12 p70 concentration

$$[\text{IL-12}] = \frac{[(\text{Absorbance at 450 nm}) - (\text{Y-intercept})] \times \text{Dilution factor}}{\text{Slope}}$$

* If samples have been diluted, the concentration read from the standard curve must be multiplied by the dilution factor.

3.3.5 Serum IL-18 assay

Serum IL-18 was determined using a commercially available mouse IL-18 ELISA Kit (Medical & Biological Laboratory Co., Ltd, Japan).

Principle of the assay: The mouse IL-18 ELISA Kit measures mouse IL-18 by sandwich ELISA. The assay uses two monoclonal antibodies against two different epitopes of mouse IL-18. In the wells coated with anti-mouse IL-18 monoclonal antibody, samples to be measured or standards are incubated. After washing, a peroxidase conjugated anti-mouse IL-18 monoclonal antibody is added into the microwell and incubated. After another washing, the peroxidase substrate is mixed with the chromogen and allowed to incubate for an additional period of time. An acid solution is then added to each well to terminate the enzyme reaction and to stabilize the developed color. The O.D. of each well is then measured at 450 nm using a microplate reader. The concentration of Mouse IL-18 is calibrated from a dose response curve based on reference standards.

Procedure: Preparation of reagents

- Wash solution**:** Prepare 1:10 dilution of the wash concentrate prior to use. (i.e., 50 mL of wash concentrate to 450 mL of distilled water). The diluted wash solution is stable for 2 weeks at 4^oC.

- Conjugate solution: Peroxidase conjugated anti-mouse IL-18 monoclonal antibody must be diluted prior to use. Dilute the peroxidase conjugated anti-mouse IL-18 monoclonal antibody 1:101 with conjugate diluents (i.e., 10 µL of the peroxidase conjugated anti-mouse IL-18 monoclonal antibody to 1000 µL of the conjugate diluents).

- Standards: Prepare fresh standards for each assay run, as the prepared standards are not stable. The prepared standards must be used within 3 hours. Reconstitute with 1.0 mL assay diluents (2500 pg/mL). Avoid repeated freezing and thawing. Dilute the 2500 pg/mL standard 1:2.5 assay diluents, and make 5 standards (1000, 400, 160, 64, and 25.6 pg/mL). Use assay diluent as 0 pg/mL standard.

- Other reagents are ready-to-use.

Standard concentration	IL-18	Assay diluent
1000 pg/mL	200 µL of 2500 pg/mL standard	300 µL
400 pg/mL	200 µL of 1000 pg/mL standard	300 µL
160 pg/mL	200 µL of 400 pg/mL standard	300 µL
64 pg/mL	200 µL of 160 pg/mL standard	300 µL
25.6 pg/mL	200 µL of 64 pg/mL standard	300 µL
Zero		300 µL

Table 3.2   Recommend dilution of the 2500 pg/mL standard with the assay diluents

Preparation of samples

- Dilution: Dilute each sample with assay diluents (i.e., Mouse serum 1:5 with assay diluents: by adding 50 µL of sample to 200 µL of assay diluents). Add 150 µL of prepared samples and standards to 96-well polyvinyl plate as the same order of assay run.

- Storage: Fresh samples should be used. Aliquote each sample into new plastic tube and store below -20^oC if necessary. Avoid repeated freezing and thawing.

Assay procedure: Duplicate assay will be recommended.

Step 1 (Sample incubation)

- Transfer 100 µL of each sample and standard to Mouse IL-18 antibody coated microwells simultaneously using multichannel pipette. Reaction starts on pipetting to Mouse IL-18 antibody coated microwell. Pipetting should be

completed as quickly as possible.

- Incubate for 60 minutes at room temperature (20-25°C).

Step 2 (Washing)

- Aspirate or discard the well contents. Fill the wells with wash solution and then completely aspirate or discard the contents. Wash the well 4 times with wash solution using washing bottle. Washing buffer should be used at room temperature (20-25°C).

Step 3 (Conjugate incubation)

- Pour conjugate solution into the vessel. After removing wash solution remained completely, pipette 100 µL of conjugate solution to each well with multichannel pipette. To avoid dry up microwells, the conjugate solution must be dispensed into the microwells as soon as remove the wash solution.

- Incubate for 60 minutes at room temperature (20-25°C).

Step 4 (Washing)

- Wash the microplate again following the step 2.

Step 5 (Substrate incubation)

- Pour substrate reagent into the vessel. Add 100 µL of substrate reagent to each well. Substrate reagent should be used at room temperature (20-25°C). This vessel should be different from the one which was used for pouring conjugate solution. Use disposable new pipette and vessel. If substrate reagent is poured into the vessel from bottle, do not return to the bottle. To avoid dry up microwells, the substrate reagent must be dispensed into the microwells as soon as remove the wash solution.

- Incubate for 30 minutes at room temperature (20-25°C).

Step 6 (Stopping reaction)

- Pour stop solution into the vessel. Pipette 100 µL of stop solution to each well with multichannel pipette.

Step 7 (Reading)

- Determine the O.D. of each well, using a microplate reader set to 450 nm. Reading should be done within 30 minutes after stopping reaction.

Calculation of results

Calculate the mean absorbance value of each standard. Plot on the semi-log graph paper and construct a standard curve (absorbance on the vertical axis, concentration (in pg/mL) on the horizontal axis). If absorbance of sample exceeds the one of the 1000 pg/mL standard, dilute the sample and measure again (Figure 3.8).
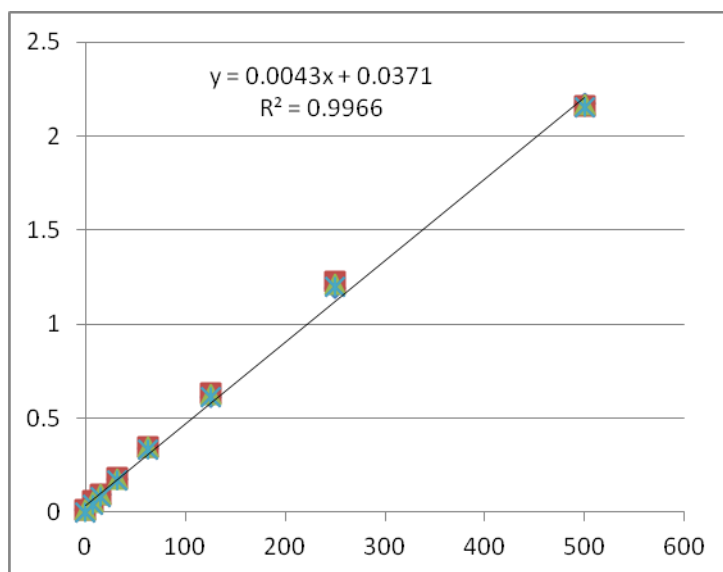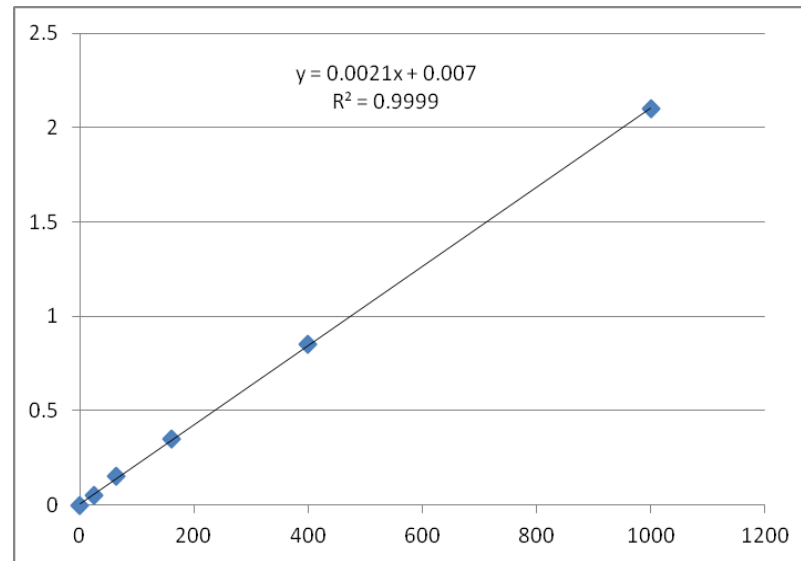
Figure 3.8   Example of standard IL-18 curve: plot of corrected absorbance at 450 nm versus IL-18 concentration

[IL-18]   = $\dfrac{\text{[(Absorbance at 450 nm)} - \text{(Y-intercept)]} \times \text{Dilution factor}}{\text{Slope}}$

     * If samples have been diluted, the concentration read from the standard curve must be multiplied by the dilution factor.

3.3.6 Histological Examination
Preparation for liver pathology

     - Tissue fixation: Immerse tissue in fixative (10% formalin solution) at room temperature.

     - Washing: Wash in 50% ethanol for 15 minutes at room temperature.

     - Dehydration: Immerse the tissue in grade series of ethanol from low to high% (70%, 80%, 95%, and 100%) for 15-30 minutes, twice each.

     - Clearing and infiltration: Immerse the tissue in xylene for 15-30 minutes at room temperature, twice, immerse in soft paraffin (mixture of paraffin and xylene as 1:1 ratio), incubate in warm oven at 60°C for 15-30 minutes, twice, and immerse in melting paraffin at 60°C for 15-30 minutes, twice.

     - Embedding: Embed the tissue in boat, leave for solidness.

     - Sectioning: Cut the paraffin block as 5 micrometre (µm) thickness, then mount on glass slide and dry the tissue section at 45°C for 3-6 hours.

     - Staining: Deparaffinization by placing the slide in xylene at room temperature, twice, hydration by immersing the slide in graded series of ethanol (high to low %), then immerse in distilled water before placing in Hematoxylin (H) for 10-15 minutes, washing in running tap water before double staining with Eosin (E) for 1.5-2 minutes, washing, and dehydration by dipping the slide in graded series of

ethanol (low to high %), twice each.

           - Clearing and mounting: Immerse the stained slide in xylene for 3-5 minutes, twice then mount the slide and cover glass with mounting media.

           The histological slides were evaluated under light microscope (LM) by an experienced pathologist who is blinded to the experiment. The severity of hepatic necroinflammation was graded on the basis of the extent of involved parenchyma. Each slide represented X10 and X40 magnification.

           The hepatic acinus is divided into zones 1, 2 and 3 and the hepatocytes in these zones have different metabolic functions. Zone 1 is closest to the portal triad and receives the most oxygenated blood, the cells in zone 2 have functional and morphologic characteristics and responses intermediate to between those of zones 1 and 3, while zone 3 is furthest away and receives least oxygen. Zone 3 is thus most susceptible to ischaemic injury (Figure 3.9).
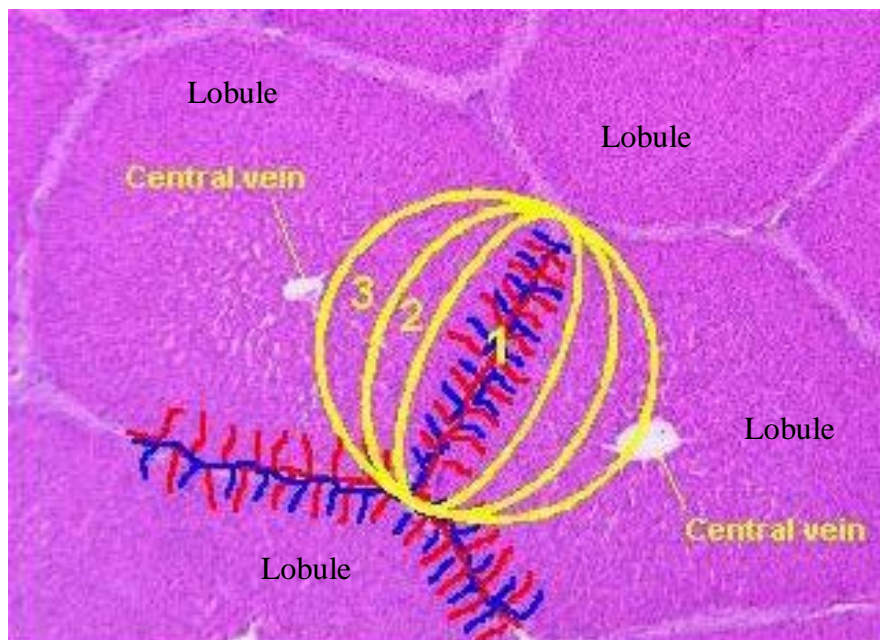
Figure 3.9   The hepatic acinus: the hepatic acinus is divided into zones 1, 2, and 3 and the hepatocytes in these zones have different metabolic functions.

           Each slide were examined for grading of hepatic necroinflammation according to the criteria described by Brunt EM et al. (68) from 0 to 3 as follow; score 0 = no hepatocyte injury/inflammation, score 1 = sparse or mild focal zone 3 hepatocyte injury/inflammation, score 2 = noticeable zone 3 hepatocyte injury/inflammation, and score 3 = severe zone 3 hepatocyte injury/inflammation.

           Cells that die due to paracetamol die in zones, which will occurred especially at zone 3, because zone 3 is furthest away, receives least oxygen, and most susceptible to ischaemic injury. When severity increases, extended throughout the zone 2 towards the zone 1 which is extensive hepatic necrosis. Therefore, in this present study we did not count the number of cells that die in each area.

3.4 Statistical analysis

All data were presented as mean and standard deviation (SD). For comparison among all groups of animals, one-way analysis of variance (one-way ANOVA) and Tukey PostHoc comparisons were employed. Differences were considered statistically significant at $p < 0.05$. The data were analyzed using the SPSS software version 17.0 for windows.

CHAPTER IV

RESULTS

4.1 The effects of curcumin on serum AST & ALT in mice with paracetamol overdose

The results of serum AST levels were presented in Table 4.1 and Figure 4.1. The serum AST in control group showed normal level (AST; 86.13±6.90 U/L). These were significantly increased in APAP group when compared with control group (AST; 583.25±118.30 vs 86.13±6.90 U/L, $p < 0.001$) and significantly decreased in APAP + CUR 200 (AST; 197.38±14.39 vs 538.25±118.30 U/L, $p < 0.001$) and APAP + CUR 600 groups (AST; 111.38±8.33 vs 583.25±118.30 U/L, $p < 0.001$) when compared with APAP group. In addition, there was significant difference between the APAP + CUR 200 and APAP + CUR 600 groups (197.38±14.39 vs 111.38±8.33 U/L, $p < 0.05$).

The results of serum ALT levels were presented in Table 4.1 and Figure 4.2. The serum ALT in control group showed normal level (ALT; 42.63±6.95 U/L). These were significantly increased in APAP group when compared with control group (ALT; 186.00±43.73 vs 42.63±6.95 U/L, $p < 0.001$) and significantly decreased in APAP + CUR 200 (ALT; 65.25±3.11 vs 186.00±43.73 U/L, $p < 0.001$) and APAP + CUR 600 groups (ALT; 47.50±4.72 vs 186.00±43.73 U/L, $p < 0.001$) when compared with APAP group. In addition, there was no significant difference between the APAP + CUR 200 and APAP + CUR 600 groups (65.25±3.11 vs 47.50±4.72 U/L, $p > 0.05$).

4.2 The effects of curcumin on hepatic GSH in mice with paracetamol overdose

The results of hepatic GSH levels were presented in Table 4.1 and Figure 4.3. Hepatic GSH in control group showed normal level (10.17±0.11 nmol/mg protein). These were significantly decreased in APAP group when compared with control group (2.75±0.16 vs 10.17±0.11 nmol/mg protein, $p < 0.001$) and significantly increased in APAP + CUR 200 (9.16±0.49 vs 2.75±0.16 nmol/mg protein, $p < 0.001$) and APAP + CUR 600 groups (9.72±0.22 vs 2.75±0.16 nmol/mg protein, $p < 0.001$) when compared with APAP group. In addition, there was significant difference between the APAP + CUR 200 and APAP + CUR 600 groups (9.16±0.49 vs 9.72±0.22 nmol/mg protein, $p < 0.05$).

4.3 The effects of curcumin on hepatic MDA in mice with paracetamol overdose

The results of hepatic MDA levels were presented in Table 4.1 and Figure 4.4. Hepatic MDA in control group showed normal level (1.45±0.01 nmol/mg protein). These were significantly increased in APAP group when compared with control group (3.55±0.05 vs 1.45±0.01 nmol/mg protein, $p < 0.001$) and significantly decreased in APAP + CUR 200 (1.47±0.01 vs 3.55±0.05 nmol/mg protein, $p < 0.001$) and APAP + CUR 600 groups (1.46±0.01 vs 3.55±0.05 nmol/mg protein, $p < 0.001$) when compared with APAP group. In addition, there was no significant difference between the APAP + CUR 200 and APAP + CUR 600 groups (1.47±0.01 vs 1.46±0.01 nmol/mg protein, $p > 0.05$).

4.4 The effects of curcumin on serum IL-12 & IL-18 in mice with paracetamol overdose

The results of serum IL-12 levels were presented in Table 4.1 and Figure 4.5. Serum IL-12 in control group showed normal level (7.08 ± 1.40 pg/mL). These were significantly increased in APAP group when compared with control group (29.16 ± 3.34 *vs* 7.08 ± 1.40 pg/mL, $p < 0.001$) and significantly decreased in APAP + CUR 200 (11.60 ± 1.68 *vs* 29.16 ± 3.34 pg/mL, $p < 0.001$) and APAP + CUR 600 groups (9.63 ± 1.38 *vs* 29.16 ± 3.34 pg/mL, $p < 0.001$) when compared with APAP group. In addition, there was no significant difference between the APAP + CUR 200 and APAP + CUR 600 groups (11.60 ± 1.68 *vs* 9.63 ± 1.38 pg/mL, $p > 0.05$).

The results of serum IL-18 levels were presented in Table 4.1 and Figure 4.6. Serum IL-18 in control group showed normal levels (29.17 ± 3.72 pg/mL). These were significantly increased in APAP group when compared with control group (139.52 ± 15.59 *vs* 29.17 ± 3.72 pg/mL, $p < 0.001$) and significantly decreased in APAP + CUR 200 (53.48 ± 18.19 *vs* 139.52 ± 15.59 pg/mL, $p < 0.001$) and APAP + CUR 600 groups (35.21 ± 2.18 *vs* 139.52 ± 15.59 pg/mL, $p < 0.001$) when compared with APAP group. In addition, there was significant difference between the APAP + CUR 200 and APAP + CUR 600 groups (53.48 ± 18.19 *vs* 35.21 ± 2.18 pg/mL, $p < 0.05$).

4.5 The effects of curcumin on liver pathology in mice with paracetamol overdose

The summarized scores of hepatic necroinflammation were presented in Table 4.2. There was no hepatocyte injury/inflammation in control group. Most mice in APAP group showed severe hepatocyte injury/inflammation with score 3. The improvement of liver pathology revealed in APAP + CUR 200 and APAP + CUR 600 groups. Most mice in these groups did not develop any hepatic necroinflammation.

Figure 4.7 illustrated the histological examination of liver from each group. Control group showed normal hepatic architecture composed of cords of hepatocytes radiating from the central vein. The hepatocytes appeared polyhedral in shape with well-defined boundaries and abundant acidophilic cytoplasm. Each cell exhibited a round vesicular, centrally located nucleus. Between cell cords, hepatic sinusoids appeared as narrow space lined with flattened endothelial cells and Kupffer cells (Figure 4.7A). In contrast, APAP group showed extensive hemorrhagic hepatic necrosis involving all zones. The necrosis, although surrounding the centrilobular areas, extended throughout the mid-zone towards the peripheral part, and eosinophilic degeneration of the cells, together with pyknotic nuclei within the central parts of the lobules. Vacuolation and early degenerative features of the more peripherally placed cells surrounding the portal tracts were observed (Figure 4.7B). In APAP + CUR 200 group showed moderate, focal necrosis, and the classical hepatic architecture of the rest of liver parenchyma was preserved (Figure 4.7C), whereas the majority of hepatic lobules preserved the normal architecture with limited hepatic change was characterized in APAP + CUR 600 group (Figure 4.7D).

Table 4.1: The effects of curcumin on hepatitis in mice with paracetamol overdose.

Group	n	Parameters					
		AST (U/L)	ALT (U/L)	GSH (nmol/mg protein)	MDA (nmol/mg protein)	IL-12 (pg/mL)	IL-18 (pg/mL)
Control	8	86.13 ± 6.90	42.63 ± 6.95	10.17 ± 0.11	1.45 ± 0.01	7.08 ± 1.40	29.17 ± 3.72
APAP	8	583.25 ± 118.30^{a1}	186.00 ± 43.73^{a1}	2.75 ± 0.16^{a1}	3.55 ± 0.05^{a1}	29.16 ± 3.34^{a1}	139.52 ± 15.59^{a1}
APAP + CUR 200	8	$197.38\pm14.39^{a2, b}$	65.25 ± 3.11^{b}	$9.16\pm0.49^{a2, b}$	1.47 ± 0.01^{b}	$11.60\pm1.68^{a2, b}$	$53.48\pm18.19^{a2, b}$
APAP + CUR 600	8	$111.38\pm8.33^{b, c}$	47.50 ± 4.72^{b}	$9.72\pm0.22^{a2, b, c}$	1.46 ± 0.01^{b}	9.63 ± 1.38^{b}	$35.21\pm2.18^{b, c}$

Results are expressed as mean ± SD; n = 8 for each group.
[a1]$p < 0.001$ and [a2]$p < 0.01$ compare with control group, [b]$p < 0.001$ compare with APAP group, and [c]$p < 0.05$, compare with APAP + CUR 200 group.
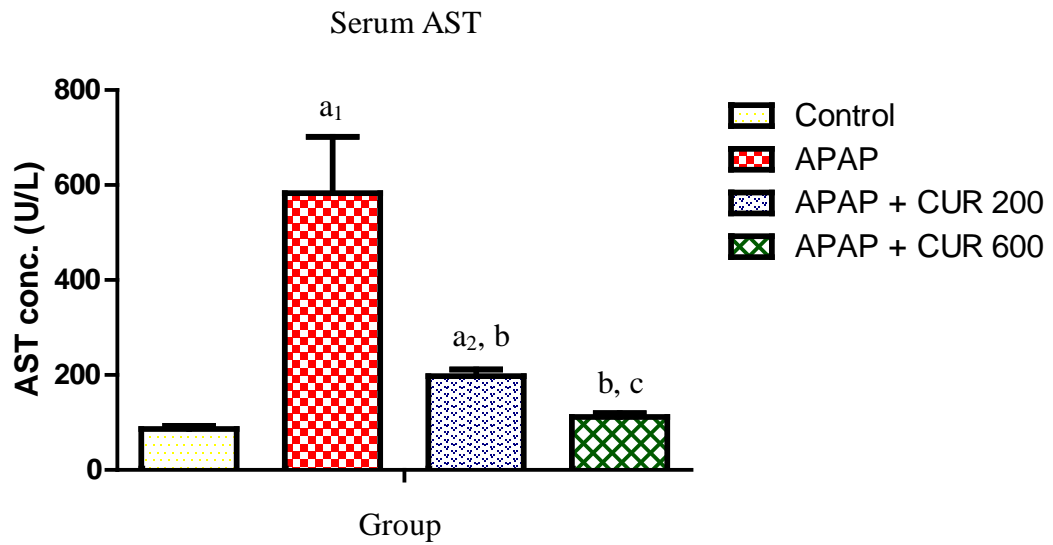
Figure 4.1: The effects of curcumin on hepatic enzyme (AST) in mice with paracetamol overdose. [a1]$p < 0.001$ and [a2]$p < 0.01$ compare with control group, [b]$p < 0.001$ compare with APAP group, and [c]$p < 0.05$, compare with APAP + CUR 200 group.
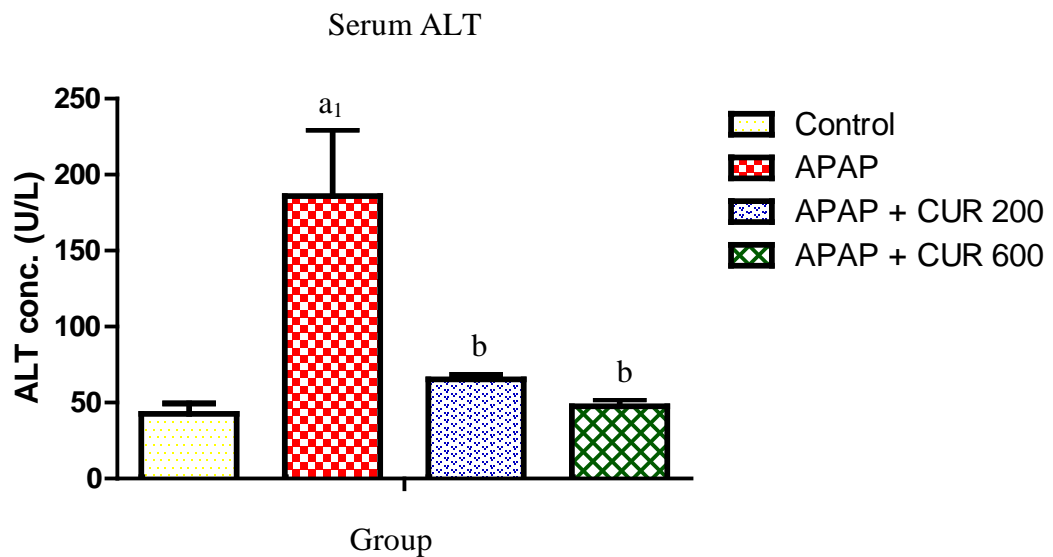
Figure 4.2: The effects of curcumin on hepatic enzyme (ALT) in mice with paracetamol overdose. [a1]$p < 0.001$ compare with control group, [b]$p < 0.001$ compare with APAP group.
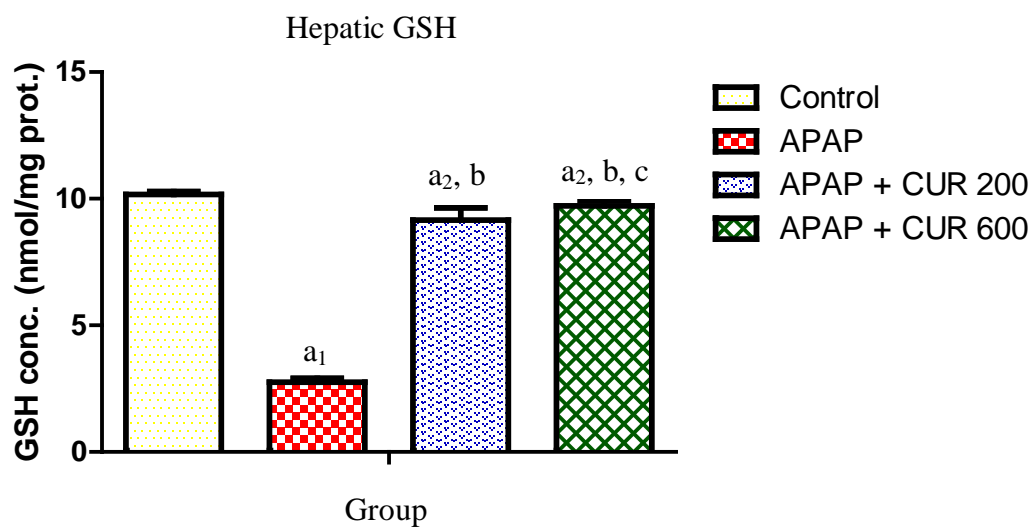
Hepatic GSH

Figure 4.3: The effects of curcumin on hepatic GSH in mice with paracetamol overdose. [a1]$p < 0.001$ and [a2]$p < 0.01$ compare with control group, [b]$p < 0.001$ compare with APAP group, and [c]$p < 0.05$, compare with APAP + CUR 200 group.
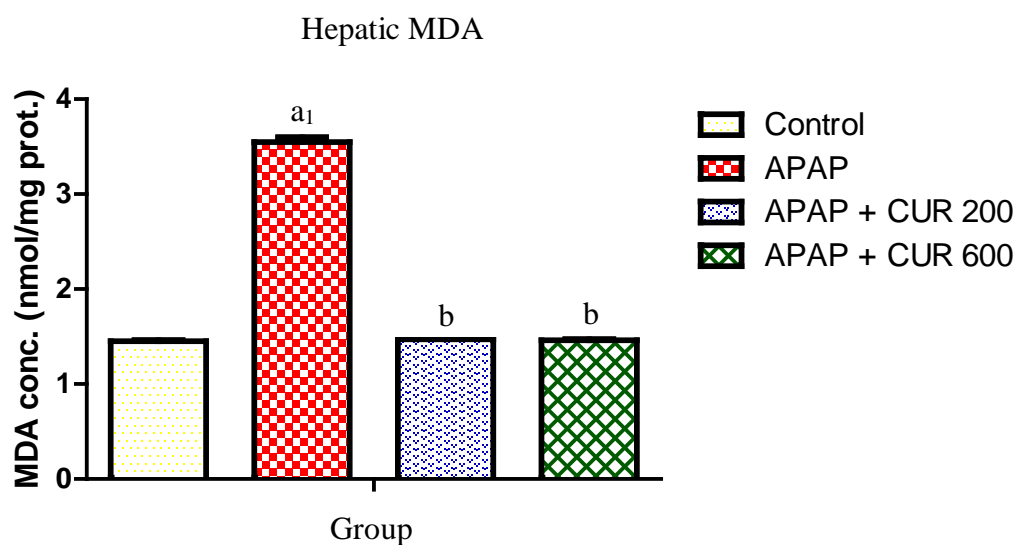
Hepatic MDA

Figure 4.4: The effects of curcumin on hepatic MDA in mice with paracetamol overdose. [a1]$p < 0.001$ compare with control group, [b]$p < 0.001$ compare with APAP group.
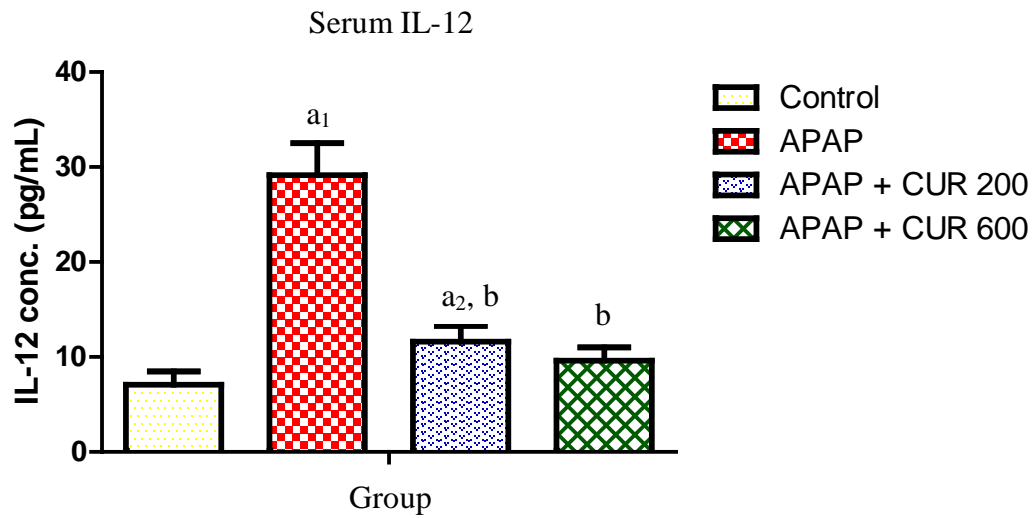
Figure 4.5: The effects of curcumin on serum IL-12 in mice with paracetamol overdose. $^{a_1}p < 0.001$ and $^{a_2}p < 0.01$ compare with control group, $^{b}p < 0.001$ compare with APAP group.
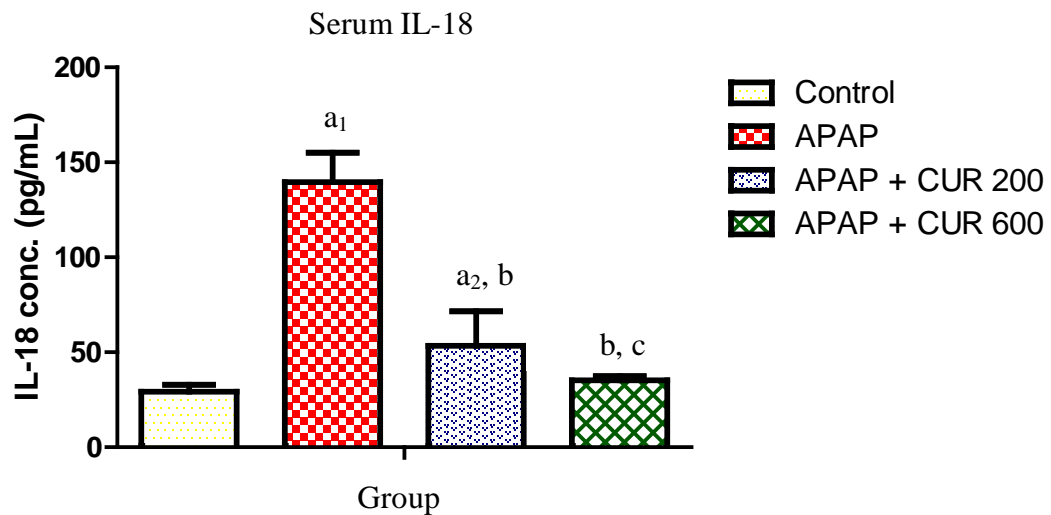
Figure 4.6: The effects of curcumin on serum IL-18 in mice with paracetamol overdose. $^{a_1}p < 0.001$ and $^{a_2}p < 0.01$ compare with control group, $^{b}p < 0.001$ compare with APAP group, and $^{c}p < 0.05$, compare with APAP + CUR 200 group.

Table 4.2: Summarized scores of hepatic necroinflammation.

Group	Number	Hepatic necroinflammation scores			
		0 = none	1 = mild	2 = moderate	3 = severe
Control	8	8	-	-	-
APAP	8	-	1	1	6
APAP + CUR 200	8	5	2	1	-
APAP + CUR 600	8	5	3	-	-

Values are number of animals.
Each section were examined for scores of hepatic necroinflammation according to the criteria described by Brunt EM et al. (68) from 0 to 3 as follow; score 0 = no hepatocyte injury/inflammation, score 1 = sparse or mild focal zone 3 hepatocyte injury/inflammation, score 2 = noticeable zone 3 hepatocyte injury/inflammation, and score 3 = severe zone 3 hepatocyte injury/inflammation.
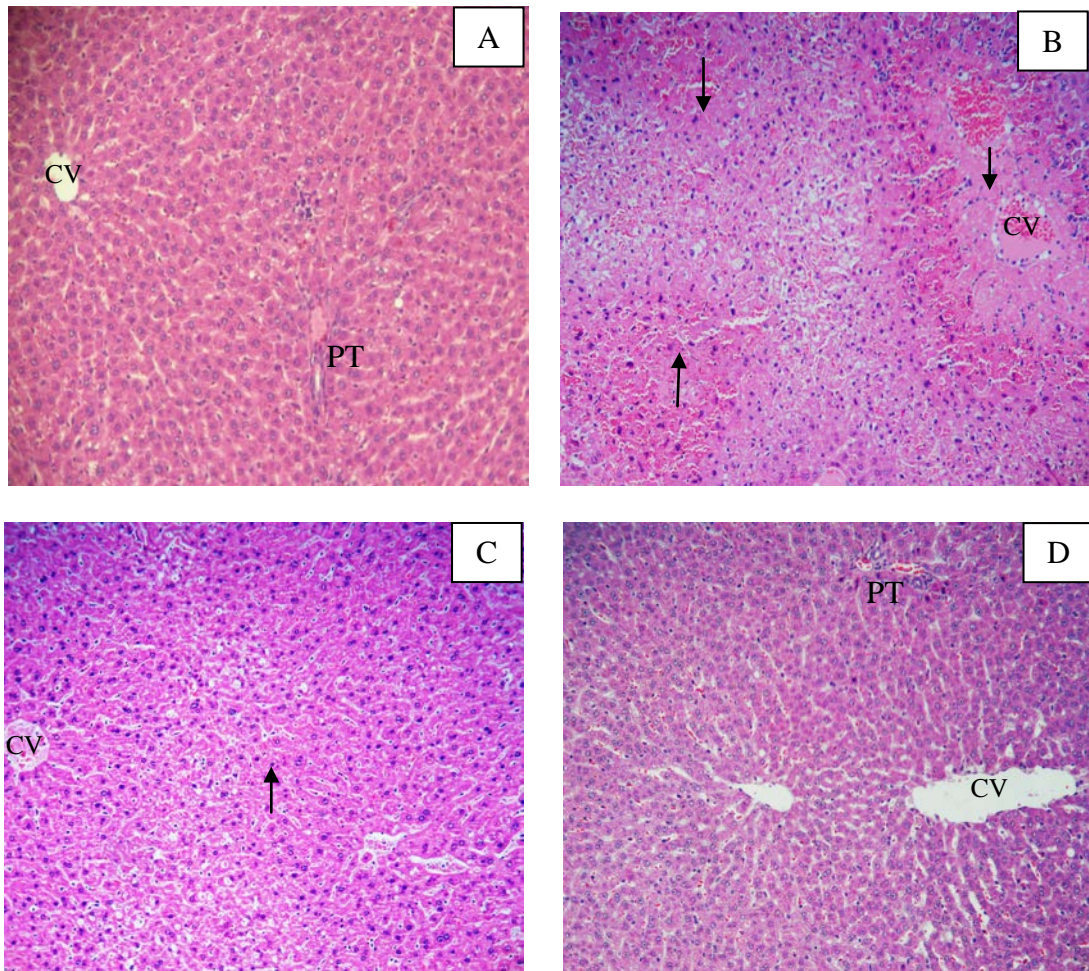
Figure 4.7: Liver histopathology of H & E staining (A); Control group showed normal hepatic architecture, (B); APAP group showed extensive hemorrhagic hepatic necrosis involving all zones, (C); APAP + CUR 200 group showed moderate, focal necrosis, and the classical hepatic architecture of the rest of liver parenchyma was preserved, and (D); APAP + CUR 600 group showed the majority of hepatic lobules preserved the normal architecture with limited hepatic change (X10). Arrows indicate hepatic necrosis, CV indicate central vein, and PT indicate portal system.
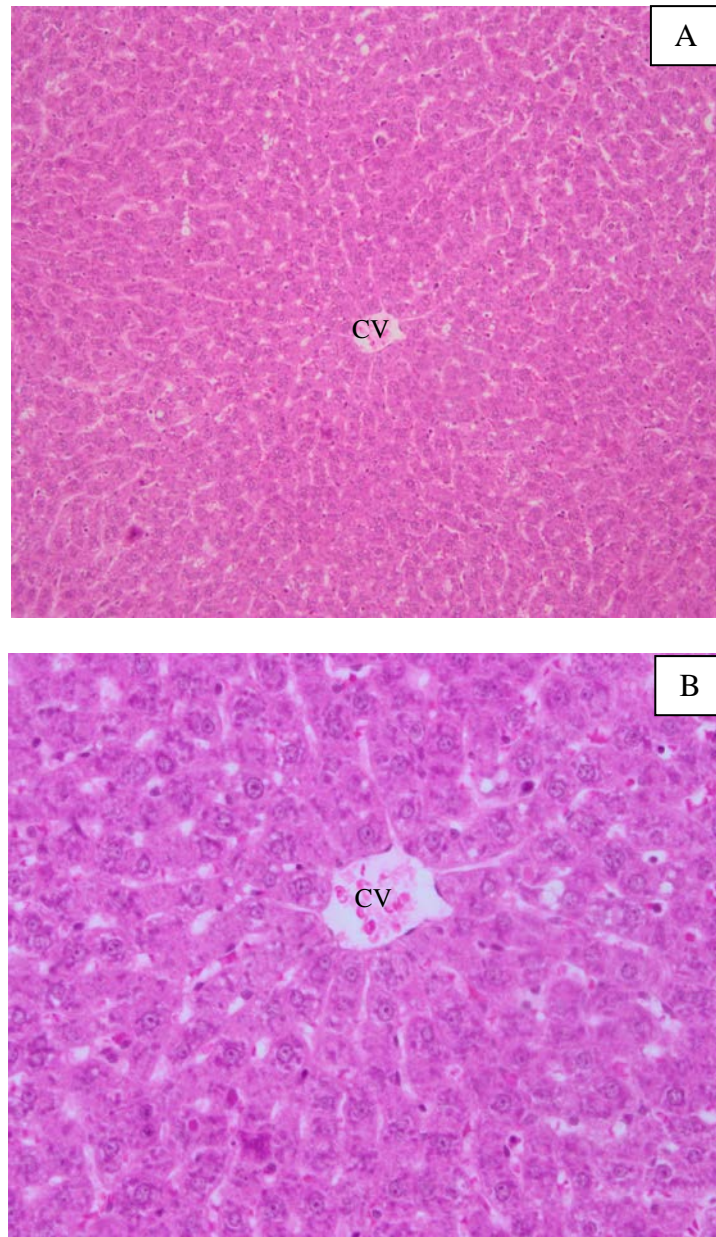
Figure 4.8: Liver histopathology of H & E staining (A and B); Control group showed normal hepatic architecture composed of cords of hepatocytes radiating from the central vein. The hepatocytes appeared polyhedral in shape with well-defined boundaries. Between cell cords, hepatic sinusoids appeared as narrow space lined with flattened endothelial cells and Kupffer cells (X10 and X40, respectively). CV indicate central vein.
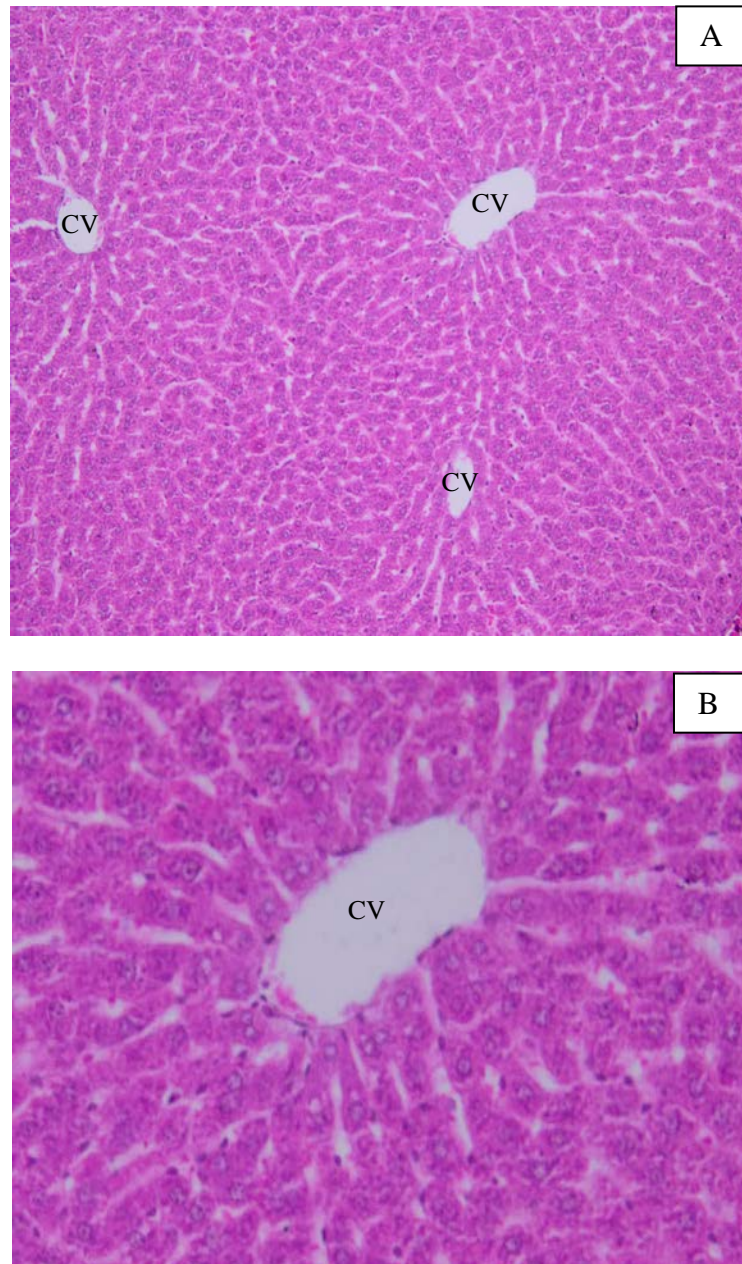
Figure 4.9: Liver histopathology of H & E staining (A and B); Control group showed normal hepatic architecture composed of cords of hepatocytes radiating from the central vein. The hepatocytes appeared polyhedral in shape with well-defined boundaries. Between cell cords, hepatic sinusoids appeared as narrow space lined with flattened endothelial cells and Kupffer cells (X10 and X40, respectively). CV indicate central vein.
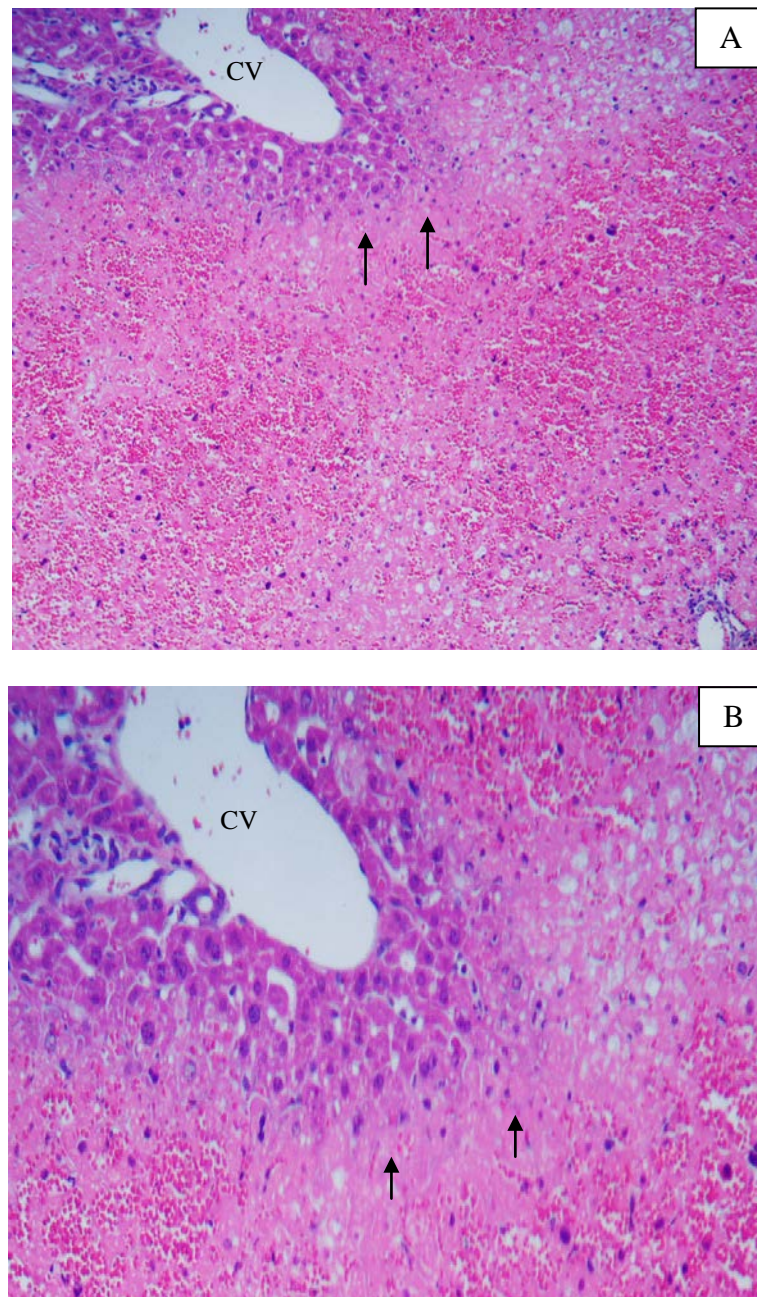
Figure 4.10: Liver histopathology of H & E staining (A and B); APAP group showed extensive hemorrhagic hepatic necrosis involving all zones. The necrosis, although surrounding the centrilobular areas, extended throughout the mid-zone towards the peripheral part, eosinophilic degeneration of the cells, and pyknotic nuclei within the lobules (X10 and X40, respectively). Arrows indicate hepatic necrosis and CV indicate central vein.
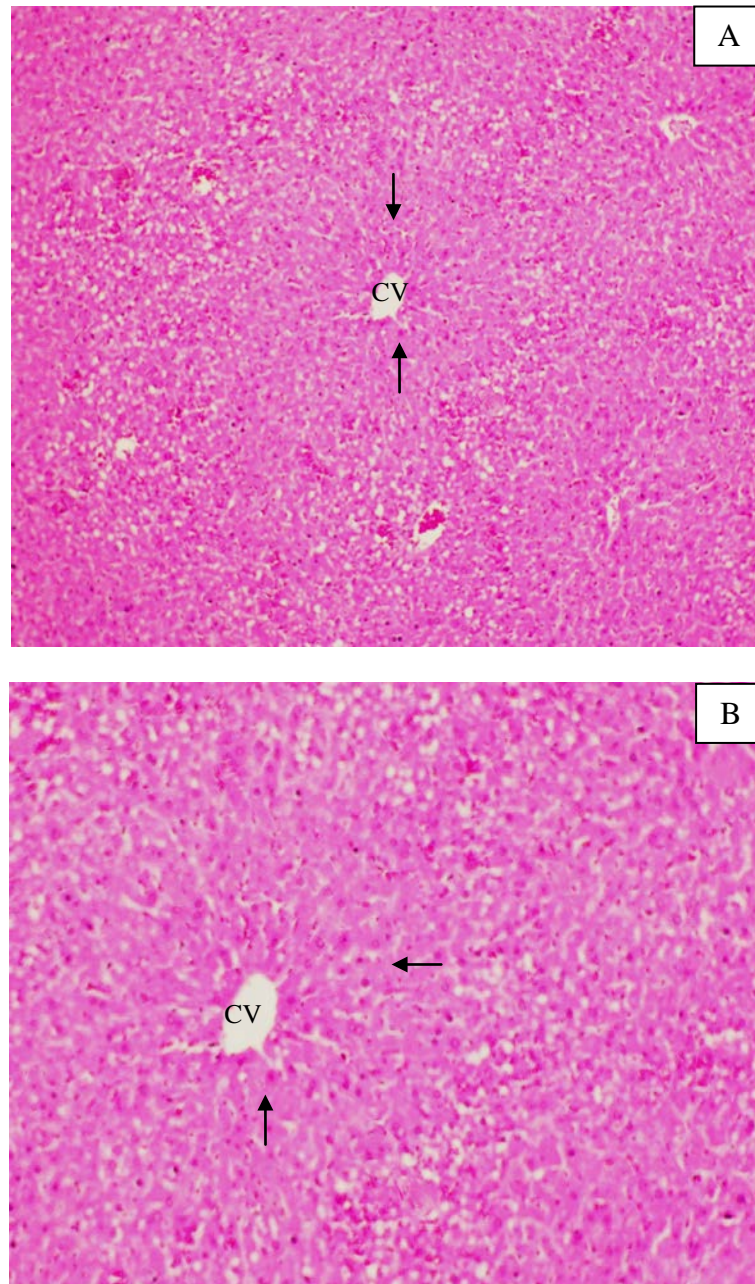
Figure 4.11: Liver histopathology of H & E staining (A and B); APAP group showed extensive hemorrhagic hepatic necrosis involving all zones. The necrosis, although surrounding the centrilobular areas, extended throughout the mid-zone towards the peripheral part, eosinophilic degeneration of the cells, and pyknotic nuclei within the lobules (X10 and X40, respectively). Arrows indicate hepatic necrosis and CV indicate central vein.
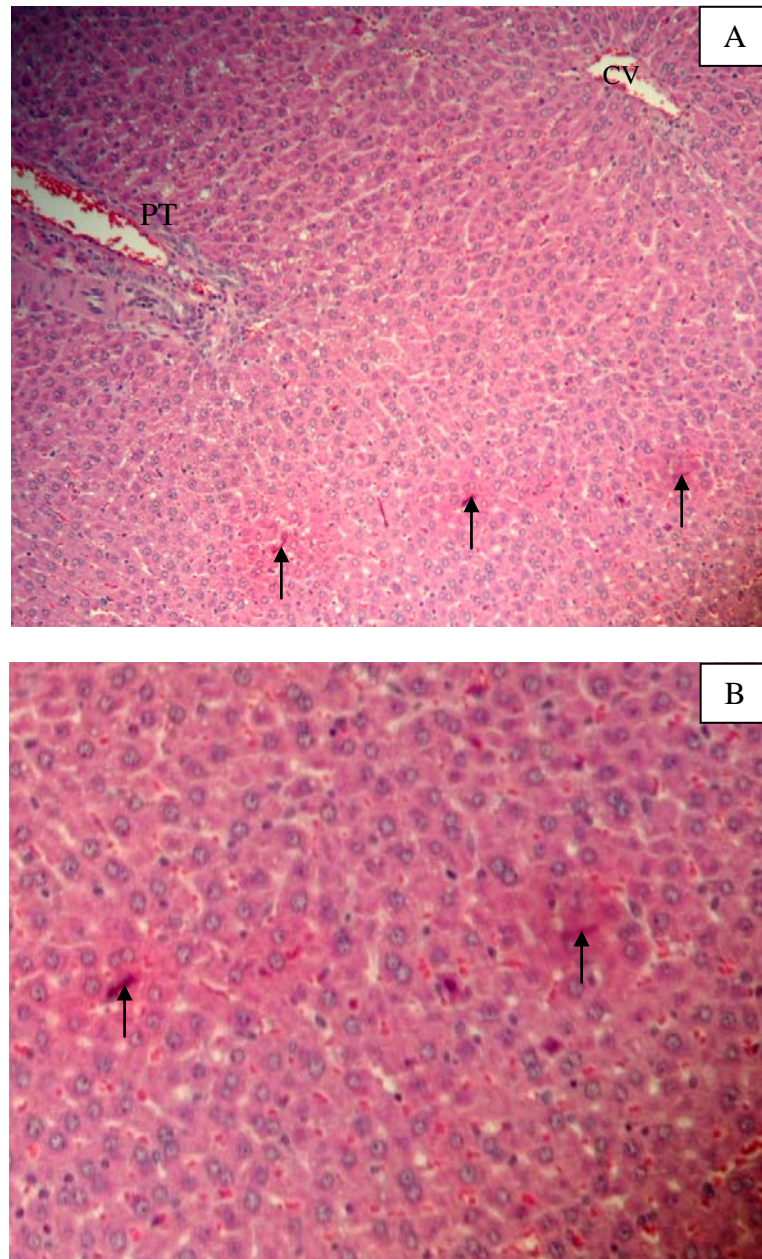
Figure 4.12: Liver histopathology of H & E staining (A and B); APAP + CUR 200 group showed mild focal necrosis and the classical hepatic architecture of the rest of liver parenchyma was preserved (X10 and X40, respectively). Arrows indicate hepatic necrosis, CV indicate central vein, and PT indicate portal system.
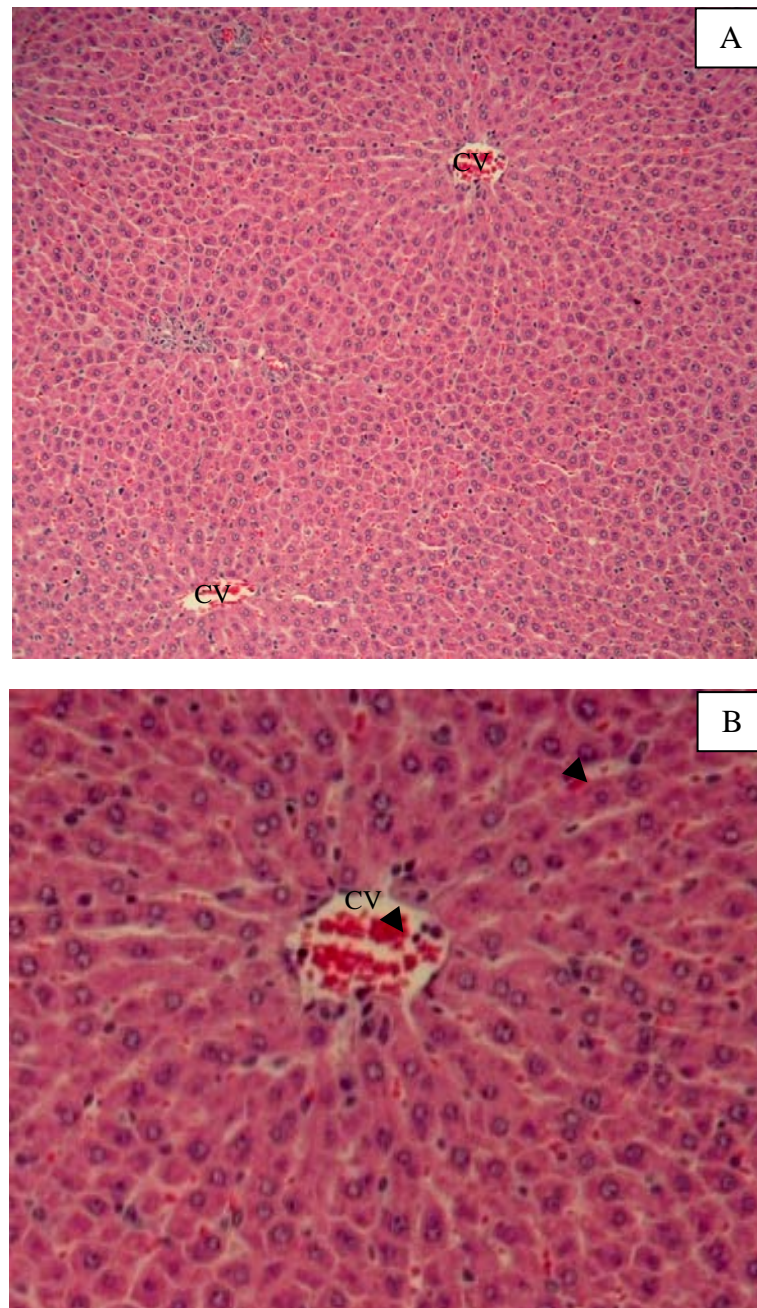
Figure 4.13: Liver histopathology of H & E staining (A and B); APAP + CUR 200 group showed diffuse congestion and the classical hepatic architecture of the rest of liver parenchyma was preserved (X10 and X40, respectively). CV indicate central vein and arrow heads indicate diffuse congestion.
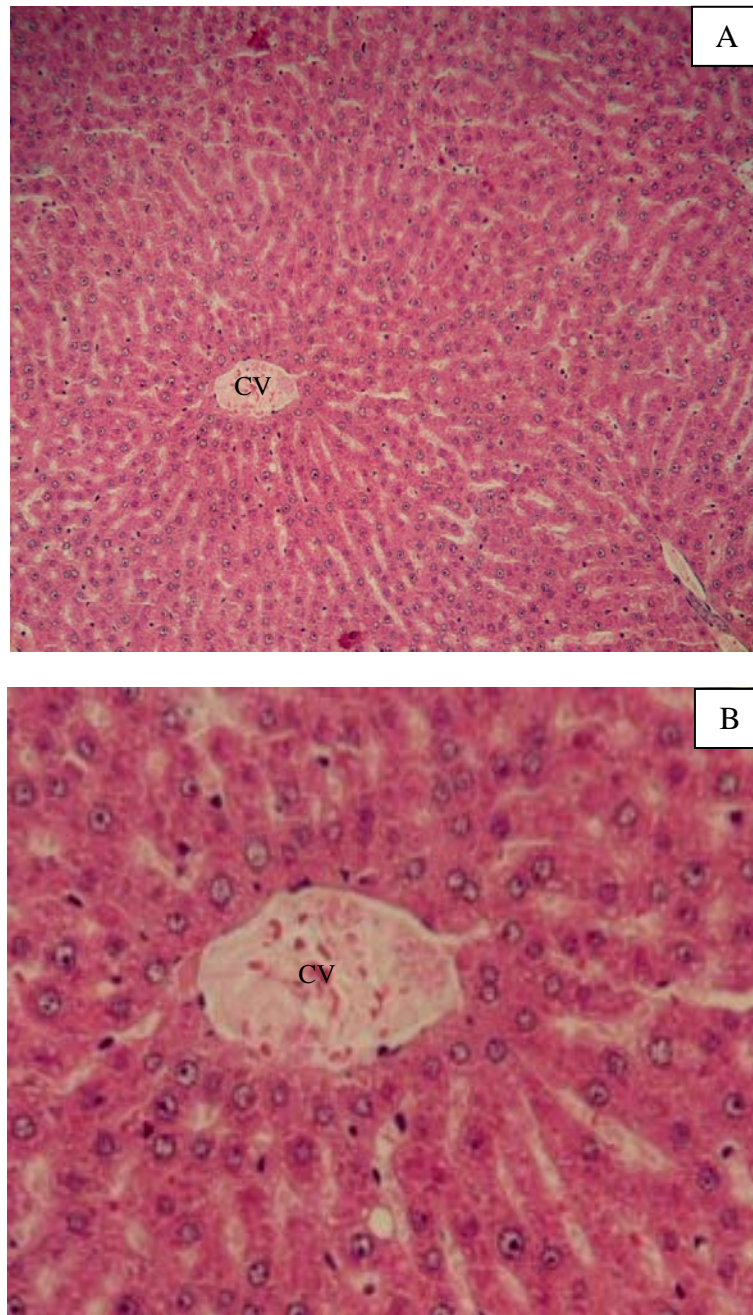
Figure 4.14: Liver histopathology of H & E staining (A and B); APAP + CUR 600 group showed normal hepatic architecture composed of cords of hepatocytes radiating from the central vein. The hepatocytes appeared polyhedral in shape with well-defined boundaries. Between cell cords, hepatic sinusoids appeared as narrow space lined with flattened endothelial cells and Kupffer cells (X10 and X40, respectively). CV indicate central vein.
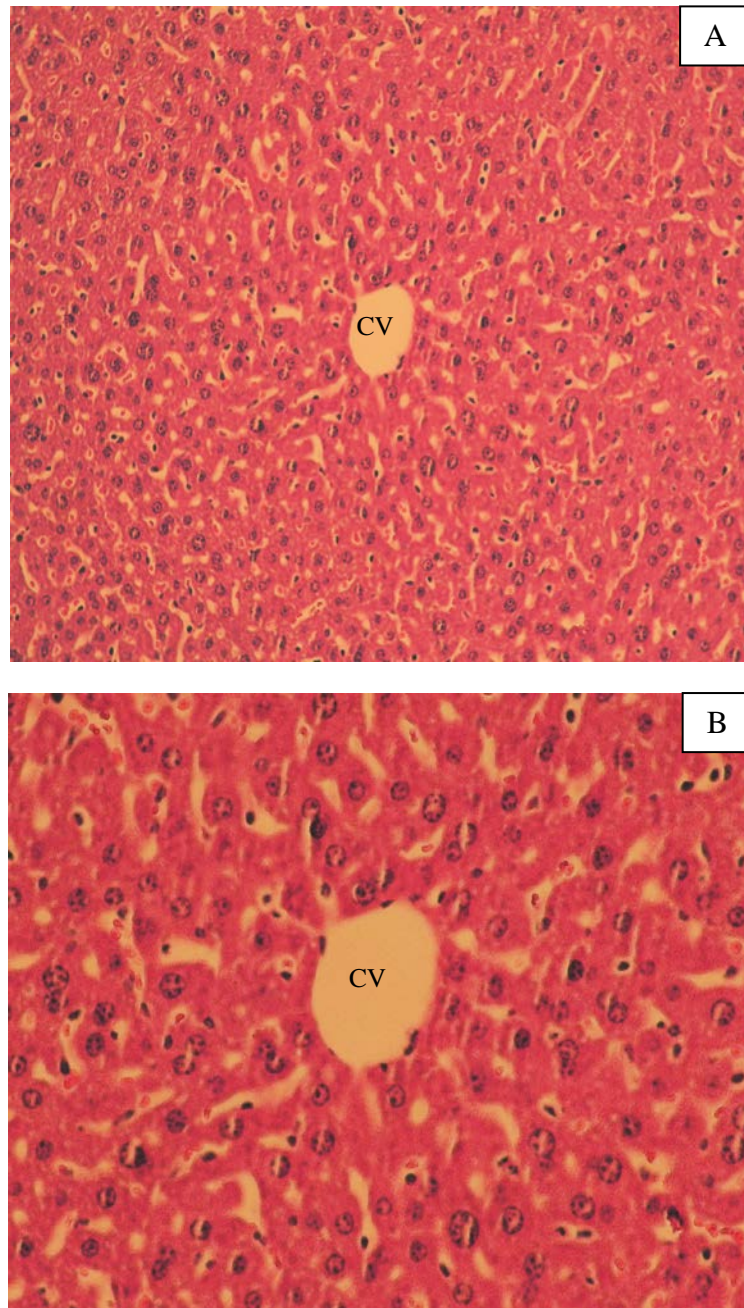
Figure 4.15: Liver histopathology of H & E staining (A and B); APAP + CUR 600 group showed normal hepatic architecture composed of cords of hepatocytes radiating from the central vein. The hepatocytes appeared polyhedral in shape with well-defined boundaries. Between cell cords, hepatic sinusoids appeared as narrow space lined with flattened endothelial cells and Kupffer cells (X10 and X40, respectively). CV indicate central vein.

CHAPTER V

DISCUSSION AND CONCLUSIONS

The present study found that increased hepatic MDA, hepatic enzymes, serum IL-12 and IL-18, decreased hepatic GSH, and the damage of liver pathology in mice with APAP overdose. Curcumin treatments resulted in decreasing the elevation of hepatic MDA, hepatic enzymes, serum IL-12 and IL-18, restoring hepatic GSH, and improving liver pathology.

The effect of paracetamol overdose on hepatic enzymes (serum AST and ALT) in mice

Hepatic enzymes are very sensitive markers employed in the diagnosis of liver disease. When the hepatocellular plasma membrane is damaged, these enzymes normally present in the cytosol are released into the blood stream. This can be quantified to assess the type and extent of liver injury (72). A number of experimental studies have demonstrated that APAP overdose increased hepatic enzymes (60-62). We found an increase in hepatic enzymes levels in APAP group. This result was similar to other previous studies.

The effect of paracetamol overdose on hepatic GSH in mice

GSH is the most important molecule against chemically induced toxicity and can participate in the elimination of toxic metabolites, by reduction of hydroperoxides in the presence of GSH dependent enzymes. It functions as a free radical scavenger, a generator of α-tocopherol and also an important role player in the maintenance of protein sulfhydryl group (73). The toxic metabolites (NAPQI) of APAP are detoxified by GSH conjugation and removed from the cells. Then, in APAP overdose causes GSH depletion and GSH depletion is a characteristic feature of hepatotoxicity (74, 75). A number of experimental studies have demonstrated that APAP overdose decreased hepatic GSH (60-62). We found a decrease in hepatic GSH level in APAP group that agreed with the previous studies.

The effect of paracetamol overdose on oxidative stress (hepatic MDA) in mice

APAP-induced liver injury has been linked to oxidative stress caused by the production of reactive oxygen intermediates. One of the characteristic features of oxidative stress is enhancement of lipid peroxidation. A number of experimental studies have demonstrated that APAP overdose increased the formation of lipid peroxidation product, such as MDA (60-62). We found an increase in hepatic MDA levels in APAP group that agreed with the previous studies.

The effect of paracetamol overdose on inflammation (serum IL-12 and IL-18) in mice

Inflammatory cytokines, mainly IL-12 and IL-18 are produced by Kupffer cells or hepatic macrophages and other inflammatory cells and have multiple effects on T lymphocytes and NK cells. Some of these effects include the induction of IFN-γ and TNF production by these cells. IL-18 shares functional similarities with IL-12 and in combination with IL-12 is strongly induced production of IFN-γ and TNF by these

cells (21-30). APAP toxicity occurred with activation of Kupffer cells indicated that Kupffer cells activation led to increase in inflammatory cytokines. These cytokines have important functions in immunity, inflammation, cell proliferation, differentiation, and cell death (57). A number of experimental studies in human and animal models have demonstrated that IL-12 and IL-18 levels were significantly increased in other diseases and liver diseases. Lissoni P et al. reported that serum IL-12 level was significantly increased in patients with metastatic renal cell carcinoma and breast cancer (76). Thong-Ngam D et al. reported that serum IL-18 level was significantly increased in patients with gastric cancer (77). Tung KH et al. reported that serum IL-12 and IL-18 levels were significantly increased in patients with alcoholic hepatitis, alcoholic cirrhosis, and alcoholic steatosis (78). Tangkijvanich P et al. reported that serum IL-12 and IL-18 levels were significantly increased in patients with hepatocellular carcinoma (79). Li J et al. reported that serum IL-18 level was significantly increased in mice with APAP-induced hepatitis (80). As a result of activation of the ICE or Caspase-1 pathway by oxidative stress, production of mature IL-18 is increased (26). Our results showed an increased in serum IL-12 and IL-18 levels in APAP group. This result was similar to other previous studies.

The effect of paracetamol overdose on liver pathology in mice

The pathological changes of APAP range from fatty changes to hepatic necrosis and progressive cell death (60-62). In the present study, the liver in APAP group showed extensive hemorrhagic hepatic necrosis involving all zones. This result was similar to other previous studies. The induction of APAP overdose occurred in the centrilobular areas, extended throughout the mid-zone towards the peripheral part. Our results showed that APAP-induced hepatic necrosis is predominantly distributed in these zones.

The effects of curcumin on hepatitis in mice with paracetamol overdose

Curcumin is the main yellow bioactive component of turmeric (*Curcuma longa* Linn.). It has been shown to possess a wide spectrum of biological actions. These include anti-inflammatory, anti-oxidant, and anti-carcinogenic activities (4-6). The hepatoprotection of curcumin have been widely acknowledged and used in traditional medicine for treatment of inflammatory conditions such as hepatitis (7). Curcumin have shown to inhibit CYP 2E enzymatic activity in rat liver microsome, cause microsomal enzyme inhibition (59).

Curcumin is dissolved in organic solvents such as Dimethylsulfoxide (DMSO), oil, alcohol, and petroleum agents. Interestingly, curcumin has been demonstrated the safety in both human and animal.

Phase 1 clinical trials have shown that curcumin is safe event at high doses (12 g/day) in humans but exhibit poor bioavailability. Major reasons contributing to the low plasma and tissue levels of curcumin appear to be due to poor absorption, rapid metabolism, and rapid systemic elimination.

In animals, the previous study demonstrated that curcumin is rapidly metabolized and poorly absorbed in Sprague-Dawley rats. Administrating curcumin orally was made by Wahlstrom B and Blennow G (41). They demonstrated that this compound in a dose of 1 to 5 g/kg BW given to rats apparently did not cause any adverse effects and it was excreted about 75% in the feces, while traces appeared in

the urine. In addition, measurements of blood plasma levels and biliary excretion showed that curcumin was poorly absorbed by the gastrointestinal tract.
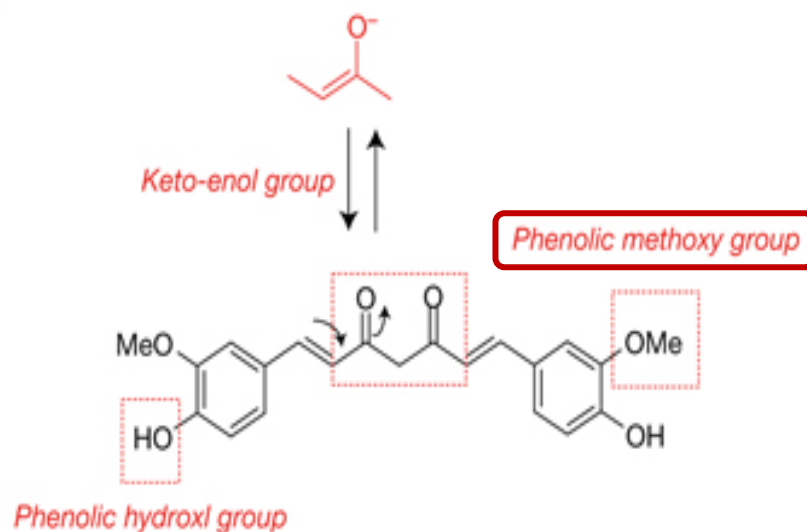
Figure 5.1   Chemical structure of curcumin and their reactive groups
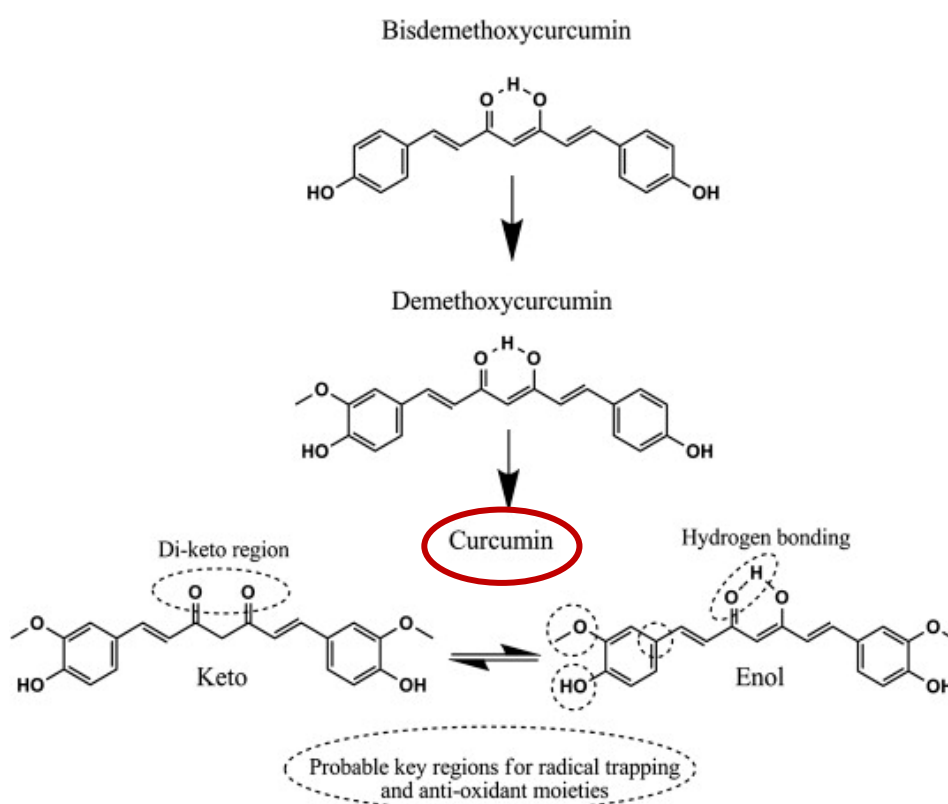
Figure 5.2   Anti-oxidant property of curcumin

The discovery of the antioxidant properties of curcumin explains many of its wide ranging pharmacological activities. The phenolic and methoxy groups on the benzene rings are important structural features that contribute to its antioxidant properties (48, 49) (Figure 5.1). The structure of curcumin, as shown in Figure 5.2, is the keto enol conformation. This probably how it exists in polar solvents and increasing solvent polarity would be expected to favor the keto-enol tautomer. Curcumin is an effective antioxidant and scavenges superoxide radical (O_2^-), hydrogen peroxide radical (H_2O_2), and nitric oxide from activated macrophages (50). It inhibited the iNOS activity in macrophages (51).

Our results showed curcumin treatments decreased oxidative stress, hepatic enzymes, reduced liver inflammation, restored hepatic GSH, and improved liver pathology in mice with APAP overdose. The protective action of curcumin can be mainly explained by GSH inducer through induction of glutathione reductase enzyme to produce GSH (reduced form) and it is the reduced form that mainly in conjugation with toxic metabolites of APAP. It was conceivable that curcumin could protect against the free radical mediated oxidative stress by scavenging of free radical that limits lipid peroxidation involved in membrane damage and stabilizing actions on cell membranes in mice with APAP overdose.
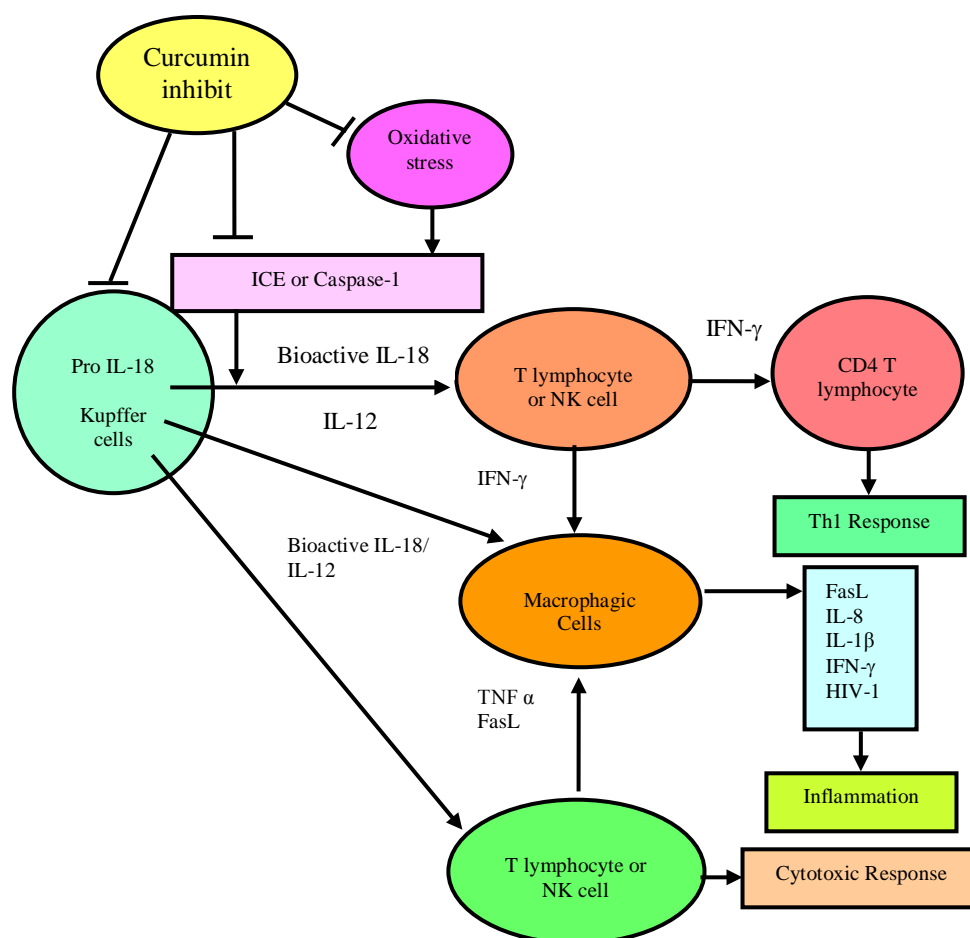
Figure 5.3   Anti-inflammatory property of curcumin

It has been reported that IL-12 is produced by dendritic cells, monocytes, Langerhans cells, neutrophils, and keratinocytes. IL-18 is produced by activated macrophages, keratinocytes, intestinal epithelial cells, osteoblasts, adrenal cortex cells, and murine diencephalon. First, IL-18 is synthesized as a precursor 24 kilodalton molecule without a signal peptide and must be cleaved to produce an active molecule. IL-1 converting enzyme (ICE or Caspase-1) cleaves pro-IL-18 at aspartic acid in P1 position, producing the mature, bioactive peptide that is readily released from cells. Importantly, both of these cytokines are produced from the same type of cells, which are Kupffer cells, and are called hepatic macrophages in the liver. It may be possible that inflammation is due to hepatocytes releasing cytokines into the blood stream, allowing us to detect them using the ELISA technique. Furthermore, these two cytokines work together and have synergistic effect in the induction of other cytokines' production which cause inflammation, such as IFN-γ, which is produced from T-lymphocytes and NK cells. In which IFN-γ that was produced will have a positive feedback effect and stimulate cells that produced it, which are Kupffer cells and inflammatory cells. Furthermore, IFN-γ stimulates CD4 T-lymphocyte causing a Th1 response and cytotoxic response. Apart from IFN-γ, T-lymphocytes and NK cells can also produce other cytokines such as TNF-α and FasL and these cytokines will stimulate macrophagic cells to produce FasL, IL-8, IL-1β, IFN-γ, and HIV-1 which will ultimately cause inflammation. Therefore, a stimulation of Kupffer cells and inflammatory cells causes an increased capacity of these cells to produce IL-18 in the form of bioactive IL-18 through ICE or Caspase-1 pathway which is the ready-to-function form, or increase the ability of these cells to produce IL-12 to work together with IL-18, finally causing an inflammation (Figure 5.3).

Curcumin is modulated the inflammatory response by down-regulating the activity of COX-2, iNOS, TNF-α, IL-1, IL-2, IL-6, and IL-8 (58). These showed that curcumin is an anti-inflammatory substance because it can inhibit the activation of the major inflammatory cytokines. These cytokines required for the expression of many cells linked with immune response.

However, there are no experiments which study the effect of curcumin in the prevention or treatment of hepatitis resulting from paracetamol overdose towards the levels of cytokines IL-12 and IL-18 which are markers of inflammation. Therefore in our experiment, we are interested in studying the effect of curcumin on hepatitis resulting from paracetamol overdose towards the levels of these cytokines to create new knowledge from this experiment. Our study shows that apart from other cytokines (such as, COX-2, iNOS, TNF-α, IL-1, IL-2, IL-6, and IL-8) that have been reported from previous studies, we show that curcumin can prevent hepatitis resulting from paracetamol overdose due to the decrease in IL-12 and IL-18 levels.

Our results showed that curcumin can directly inhibit Kupffer cells, other inflammatory cells, and ICE or Caspase-1 pathway. These data suggested that Kupffer cells activation could relate to the liver inflammation. As a result of activation of the ICE or Caspase-1 pathway by oxidative stress, production of bioactive IL-18 is increased (26). This could be explained that another pathway may reduce liver inflammation response that indirectly mediated by oxidative stress inhibition. These data suggested that oxidative stress activation could relate to liver inflammation (Figure 5.3).

Hepatic necroinflammation scores obtained from each group of mice show relationships or trends with these parameters: hepatic MDA, hepatic enzyme, hepatic GSH, and liver histopathology. This shows that if the score increases from 0 to 1, 2, and 3 in order, will also affect the levels of various markers of hepatitis resulting from paracetamol overdose and will also increase the severity of hepatitis.

The protective effect of curcumin appears to be dose-related and when the dose is increased from 200 mg/kg to 600 mg/kg, the efficacy of the hepatoprotective is enhanced. It is evident from hepatic GSH, which is better restored with 600 mg/kg dose. Similarly, on increasing the dose, the hepatic enzymes (AST) and serum IL-18 were also normalized, and the liver pathology was preserved.

For future studies we think about choosing curcumin at the dosage of 50 or 100 mg/kg which is lower than the dosage used in this present study. This is due to the results from this study which show that curcumin at 200 mg/kg which is a low dose in this study can prevent hepatitis resulting from paracetamol overdose.
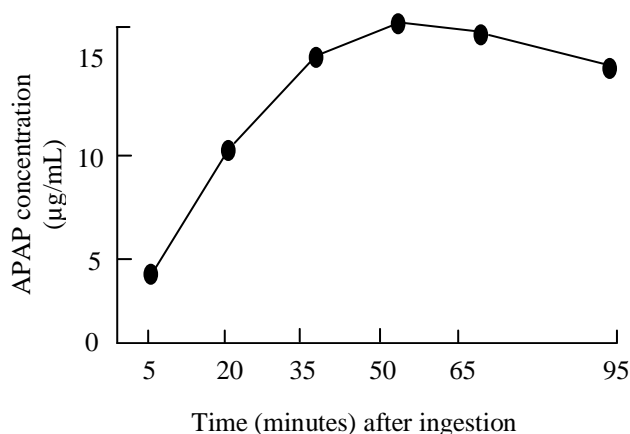
Figure 5.4   Mean plasma concentrations of APAP in subjects after single oral APAP (200 mg/kg) administration. The concentration of APAP was determined with Fluorescence Polarization Immunoassay (FPIA) (81).
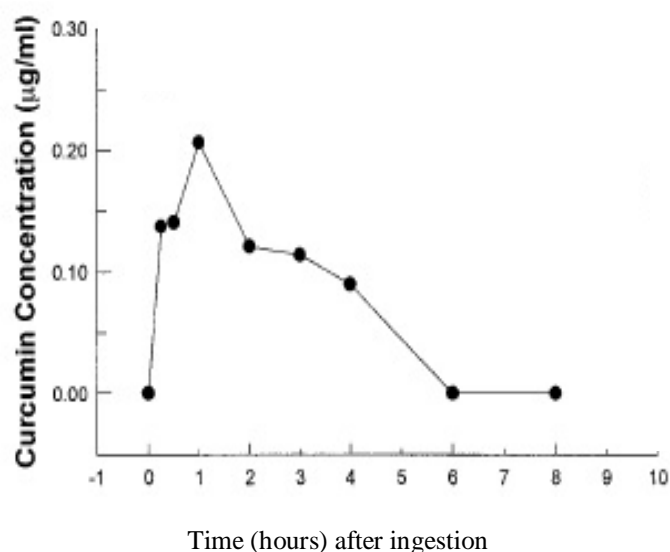
Figure 5.5   Mean plasma concentrations of curcumin in mice after single oral curcumin (1g/kg) administration. The concentration of curcumin was determined with HPLC technique (40).

Figures 5.4 and 5.5 showed mean peak plasma concentration of paracetamol and curcumin, respectively. The mean peak plasma concentration of paracetamol and curcumin occurred at 50 minutes and 1 hour after oral administration, respectively. From the data, the time required to the maximum concentration of both paracetamol and curcumin have similar values. Therefore, in this present study, curcumin is effective in preventing hepatitis resulting from paracetamol overdose.
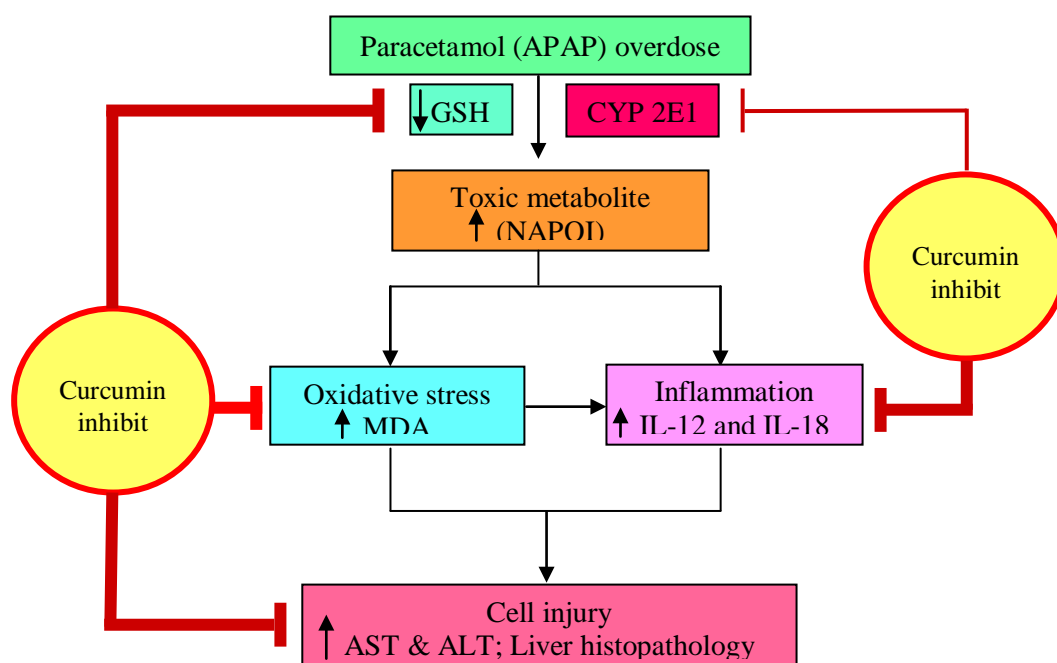
Figure 5.6   The effects of curcumin on hepatitis in mice with paracetamol overdose

In therapeutic dose, APAP is partly metabolized by CYP 2E1, to produce toxic metabolites, mainly NAPQI. Toxic metabolites produced in the liver and detoxified by GSH conjugation and removed from the cells. In APAP overdose, APAP is mainly metabolized by CYP 2E1 causes increasing of toxic metabolites and GSH depletion. These metabolites interact with biomolecules such as protein, lipid, and nucleic acid via covalent binding.

In conclusion, APAP overdose can cause liver injury. Our results show curcumin could attenuate APAP-induced liver injury by decrease oxidative stress, reduce liver inflammation, restore hepatic GSH, and improve liver pathology (Figure 5.6). In addition, curcumin at the dose of 600 mg/kg tends to be more potent than 200 mg/kg in preventing the effects of APAP hepatotoxicity. Hence, curcumin might be a novel therapeutic strategy against hepatitis caused by APAP overdose.

REFERENCES

(1)   Holt, M.P., and Ju, C. Mechanisms of Drug-Induced Liver Injury. The AAPS J
            8(2006) : 48-54.

(2)   Ostapowicz, G., et al. Results of a Prospective Study of Acute Liver Failure at
            17 Tertiary Care Centers in the United States. Ann Intern Med
            137(2002) : 947-54.

(3)   Larrey, D. Drug-induced liver diseases. J Hepatol 32(2000) : 77-88.

(4)   Maheshwari, R.K., Singh, A.K., Gaddipati, J., and Srimal. R.C. Multiple
            biological activities of curcumin: A short review. Life Sciences
            78(2006) : 2081-7.

(5)   Murathanum, R., Thong-Ngam, D., and Klaikaew, N. Curcumin Prevents
            Indomethacin-induced Acute Gastric Mucosal Damage in Rats. Thai J
            Gastroenterol 9(2008) : 118-23.

(6)   Sintara, K., Thong-Ngam, D., Patumraj, S., Klaikeaw, N., and Chatsuwan,
            T. Curcumin suppresses gastric NF-kappaB activation and
            macromolecular leakage in Helicobacter pylori infected rats. World J
            Gastroenterol 16(2010) : 4039-46.

(7)   Samuhasaneeto, S., Thong-Ngam, D., Kulaputana, O., Suyasunanont, D., and
            Klaikeaw, N. Curcumin decreased oxidative stress, inhibited
            NF-kappaB activation, and improved liver pathology in
            ethanol-induced liver injury in rats. J Biomed Biotechnol 2009
            (2009) : 1-8.

(8)   Mladenovic, D., Radosavljevic, T., Ninkovic, M., Vucevic, D.,
            Jesic-Vukicevic, R., and Todorovic V. Liver antioxidant capacity in
            the early phase of acute paracetamol-induced liver injury in mice. Food
            Chem Toxicol 47(2009) : 866-70.

(9)   Gu, J., et al. In vivo mechanisms of tissue selective drug toxicity: Effects of
            liver-specific knockout of the NADPH-cytochrome P450 reductase
            gene on acetaminophen toxicity in kidney, lung, and nasal
            mucosa. Mol Pharmacol 67(2005) : 623-30.

(10)   Hart, S.G.E., Beierschmitt, W.P., Wyand, D.S., Khairallah, E.A., and Cohen,
            S.D. Acetaminophen Nephrotoxicity in CD-1 Mice: I. Evidence of a
            Role for in Situ Activation in Selective Covalent Binding and
            Toxicity. Toxicol Appl Pharmacol 126(1994) : 267-75.

(11)   Bessems, J.G.M., and Vermeulen, N.P.E.. Paracetamol (Acetaminophen)-
            Induced Toxicity: Molecular and Biochemical Mechanisms, Analogues
            and Protective Approaches. Crit Rev Toxicol 31(2001) : 55-138.

(12)   Reppaport, A.M. Anatomic considerations. 4th ed. pp. 1-49. Philadelphia,
            1956.

(13)   Ross, M.H., Kaye, G.I., and Pawlina, W. Histology A text and atlas. 4th ed. pp.
            535-539. The United States : Lippincott Williams & Wilkins, 2003.

(14)   Tortora, G.J., and Grabowski, S.R. Principles of anatomy and physiology. 9th
            ed. pp. 843-845. The United States : John Witey & Sons, 2000.

(15)   Romanes, G.J. Cunningham's mannual of practical anatomy. Volume two
            thrax and abdomen. 15th ed. pp. 115. The United States: Oxford
            Medical Publications, 1986.

(16)   Renner, E.L. Liver function test. Baillieres Clin Gastroenterol 9(1995) : 661-7.

(17) Loeckie, L., Zwart, D.E., John, H.N.M., Jan, N.M.C., and PEV, N. Biomarker of free radical damage applications in experimental animals and humans. Free Radic Biol Med 26(1999) : 202-26.

(18) Kobayashi, M., et al. Identification and purification of natural killer cell stimulatory factor (NKSF), a cytokine with multiple biologic effects on human lymphocytes. J Exp Med 170(1989) : 827-45.

(19) Stern, A.S., et al. Purification to homogeneity and partial characterization of cytotoxic lymphocyte maturation factor from human B-lymphoblastoid cells. Proc Natl Acad Sci USA 87(1990) : 6808-12.

(20) Gubler, U., et al. Coexpression of two distinct genes is required to generate secreted bioactive cytotoxic lymphocyte maturation factor. Proc Natl Acad Sci USA 88(1991) : 4143-7.

(21) Trinchieri, G. Interleukin-12: A proinflammatory cytokine with immunoregulatory functions that bridge innate resistance and antigen-specific adaptive immunity. Annu Rev Immunol 13(1995) : 251-76

(22) Puddu, P., et al. IL-12 induces IFN-gamma expression and secretion in mouse peritoneal macrophages. J Immunol 159(1997) : 3490-7.

(23) Windhagen, A., Anderson, D.E., Carrizosa, A., Williams, R.E., and Hafler, D.A. IL-12 induces human T cells secreting IL-10 with IFN-gamma. J Immunol 157(1996) : 1127-31.

(24) Mehrotra, P.T., et al. Production of IL-10 by human natural killer cells stimulated with IL-2 and/or IL-12. J Immunol 160(1998) : 2637-44.

(25) Wolf, S.F., Sieburth, D., and Sypek, J. Interleukin 12: A key modulator of immune function. Stem Cells 12(1994) : 154-68.

(26) Okamura, H., et al. Cloning of a new cytokine that induces IFN-gamma production by T cells. Nature 378(1995) : 88-91.

(27) Ushio, S., et al. Cloning of the cDNA for human IFN-gamma-inducing factor, expression in Escherichia coli, and studies on the biologic activities of the protein. J Immunol 156(1996) : 4274-9.

(28) Micallef, M.J., et al. Interferon gamma-inducing factor enhances T helper 1 cytokine production by stimulated human T cells: Synergism with interleukin-12 for interferon-gamma production. Eur J Immunol 26(1996) : 1647-51.

(29) Dao, T., Ohashi, K., Kayano, T., Kurimoto, M., Okamura, H. Interferon-γ-Inducing Factor, a Novel Cytokine, Enhances Fas Ligand-Mediated Cytotoxicity of Murine T Helper 1 Cells. Cell Immunol 173(1996) : 230-5.

(30) Taniguchi, M., et al. Characterization of anti-human interleukin-18 (IL-18)/interferon-gamma-inducing factor (IGIF) monoclonal antibodies and their application in the measurement of human IL-18 by ELISA. J Immunol Methods 206(1997) : 107-13.

(31) Charles, A.D. Interleukin-18. Methods 19(1999) : 121-32.

(32) Foyer, C.H, Lelandais, M., and Kunert, K.J. Photooxidative stress in plants. Physiol Plant 92(1994) : 696-717.

(33) Arias, I.M., and Jakoby, W.B. Glutathione: Metabolism and function. New York : Raven Press, 1976.

(34) Baillie, T.A., and Slatter, J.G. Glutathione: A vehicle for the transport of chemically reactive metabolites in vivo. Acc Chem Res 24(1991) : 264-70.

(35) Inoue, M., Saito, Y., Hirata, E., Morino, Y., and Nagase, S. Regulation of redox states of plasma proteins by metabolism and transport of glutathione and related compounds. J Protein Chem 6(1987) : 207-25.

(36) Inoue, M. In Renal Biochemistry. In Kinne RKH (ed.), Interogan metabolism and membrane transport of glutathione and related compounds. pp. 225-265. London : Elsevier Science, 1985.

(37) Lash, L.H., and Jones, D.P. Distribution of oxidized and reduced forms of glutathione and cysteine in rat plasma. Arch Biochem Biophys 240(1985) : 583-92.

(38) Wendel, A., and Cikryt, P. The level and half-life of glutathione in human plasma. FEBS Lett 120(1980) : 209-11.

(39) Appiah-Opong, R., Commandeur, J.N., van Vugt-Lussenburg, B., and Vermeulen, N.P. Inhibition of human recombinant cytochrome P450s by curcumin and curcumin decomposition products. Toxicology 235(2007) : 83-91.

(40) Pan, M.H., Huang, T.M., and Lin, J.K. Biotransformation of curcumin through reduction and glucuronidation in mice. Drug Metab Dispos 27(1999) : 486-94.

(41) Wahltrom, B., and Blennow, G. A study on the fate of curcumin in the rats. Pharmacol 43(1978) : 86-92.

(42) Ravindranath, V., and Chandrasekhara, N. Absorption and tissue distribution of curcumin in rats. Toxicology 16(1980) : 259-65.

(43) Ravindranath, V., and Chandrasekhara, N. Metabolism of curcumin-studies with [^{3}H] curcumin. Toxicology 16(1982) : 259-65.

(44) Park, E.J., Jeon, C.H., Ko, G., Kim, J., and Sohn, D.H. Protective effect of curcumin in rat liver injury induced by carbon tetrachloride. J Pharm Pharmacol 52(2000) : 437-40.

(45) Ireson, C., et al. Characterization of metabolites of the chemoprotective agent curcumin in human and rat hepatocytes and in the rat in vivo, and evaluation of their ability to inhibit phorbol ester-induced prostaglandin E2 production. Cancer Res 61(2001) : 1058-64.

(46) Arora, R., Basu, N., and Kapoor, V. Anti-inflammatory studies on *Curcuma longa* (turmeric). Indian J Med Res 59(1971) : 1289-95.

(47) Cheng, A.L., et al. Phase I clinical trial of curcumin, a chemopreventive agent, in patients with high-risk or pre-malignant lesions. Anticancer Res 21(2001) : 2895-2900.

(48) Sreejayan, N., and Rao, M.N. Free radical scavenging activity of curcuminoids. Arzneimittelforschung 46(1996) : 169-71.

(49) Sreejayan, N., and Rao, M.N. Nitric oxide scavenging by curcuminoids. J Pharm Pharmacol 49(1997) : 105-7.

(50) Joe, B., and Lokesh, B.R. Role of capsaicin, curcumin and dietary n-3 fatty acids in lowering the generation of reactive oxygen species in rat peritoneal macrophages. Biochem Biophys Acta 1224(1994) : 255-63.

(51) Brouet, I., and Ohshima, H. Curcumin, anti-tumor promoter and anti-inflammatory agent, inhibits induction of nitric oxide synthase in activated macrophages. Biochem Biophys Res Commun 206(1995) : 533-40.

(52) Reddy, A.C., and Lokesh, B.R. Effect of curcumin and eugenol on iron-induced hepatic toxicity in rats. Toxicology 107(1996) : 39-45.

(53) Park, E.J., Jeon, C.H., KO, G., Kim, J., Sohn, and D.H. Protective effect of curcumin in rat liver injury induced by carbontetrachloride. J Pharm Pharmacol 52(2000) : 437-40.

(54) Reddy, A.C., and Lokesh, B.R. Effect of dietary turmeric (*Curcuma longa*) on iron-induced lipid peroxidation in rat liver. Food Chem Toxicol 32(1994) : 279-83.

(55) Chan, M.M. Inhibition of tumor necrosis factor by curcumin, a phytochemical. Biochem pharmacol 49(1995) : 1551-56.

(56) Gupta, B., and Ghosh, B. *Curcuma longa* inhibits TNF-alpha induced expression of adhesion molecules on human umbilical vein endothelial cells. Int J Immunopharmacol 21(1999) : 745-57.

(57) Hinson, J.A., Roberts, D.W, and James, L.P. Mechanisms of acetaminophen-induced liver necrosis. Handb Exp Pharmacol 196(2010) : 369-405.

(58) Jurenka, J.S. Anti-inflammatory properties of curcumin, a major constituent of Curcuma longa: A review of preclinical and clinical research. Altern Med Rev 14(2009) : 141-53.

(59) Oetari, S., Sudibyo, M., Commandeur, J.N., Samhoedi, R., and Vermeulen, N.P. Effects of curcumin on cytochrome P450 and glutathione S-transferase activities in rat liver. Biochem Pharmacol 51(1996) : 39-45.

(60) Girish, C., et al. Hepatoprotective activity of picroliv, curcumin and ellagic acid compared to silymarin on paracetamol induced liver toxicity in mice. Fundam Clin Pharmacol 23(2009) : 735-45.

(61) Kheradpezhouh, E., et al. Curcumin protects rats against acetaminophen-induced hepatorenal damages and shows synergistic activity with N-acetyl cysteine. Eur J Pharmacol 628 (2010) : 274-81.

(62) Yousef, M.I., Omar, S.A., El-Guendi, M.I., and Abdelmegid, L.A. Potential protective effects of quercetin and curcumin on paracetamol-induced histological changes, oxidative stress, impaired liver and kidney functions and haematotoxicity in rat. Food Chem Toxicol 48(2010) : 3246-61.

(63) Draper, H.H., and Hadley, M. Malondialdehyde determination as index of lipid peroxidation. Methods Enzymol 186(1990) : 421-31.

(64) Ohkawa, H., Ohishi, N., and Yagi, K. Assay for lipid peroxides in animal tissues by thiobarbituric acid reaction. Anal Biochem 95(1979) : 351-8.

(65) Tietze, F. Enzymic method for quantitative determination of nanogram amounts of total and oxidized glutathione: applications to mammalian blood and other tissues. Anal Biochem 27(1969) : 502-22.

(66) Eyer, P., and Podhradsky, D. Evaluation of the micromethod for determination of glutathione using enzymatic cycling and Ellman's reagent. Anal Biochem 153(1986) : 57-66.

(67)   Baker, M.A., Cerniglia, G.J., and Zaman, A. Microtiter plate assay for the measurement of glutathione and glutathione disulfide in large numbers of biological samples. <u>Anal Biochem</u> 190(1990) : 360-5.

(68)   Brunt, E.M., Janney, C.G., Di Bisceglie, A.M., Neuschwander-Tetri, B.A., and Bacon, BR. Nonalcoholic steatohepatitis: A proposal for grading and staging the histological lesions. <u>Am J Gastroenterol</u> 94(1999) : 2467-74.

(69)   Maddrey, W.C. Drug induced hepatotoxicity. <u>J Clin Gastroenterol</u> 39(2005) : 83-9.

(70)   Dash, D.K., et al. Evaluation of hepatoprotective and antioxidant activity of Ichnocarpus frutescens (Linn.) R.Br. on paracetamol-induced hepatotoxicity in rats. <u>Tropical J Pharmaceutical Res</u> 6(2007) : 755-65.

(71)   Xiong, X., et al. Effects of ursolic acid on liver protection and bile secretion. <u>Zhong Yao Cai</u> 26(2003) : 578-81.

(72)   Sallie, R., Tredger, J.M., and Williams, R. Drugs and the liver. Part 1: Testing liver function. <u>Biopharm Drug Dispos</u> 12(1991) : 251-9.

(73)   Meister, A. New aspects of glutathione biochemistry and transport-selective alteration of glutathione metabolism. <u>Nutr Rev</u> 42(1984) : 397-410.

(74)   Campos, R., Garrido, A., Guerra, R., and Valenzuela, A. Silybin dihemisuccinate protects against glutathione depletion and lipid peroxidation induced by acetaminophen on rat liver. <u>Planta Med</u> 55(1989) : 417-9.

(75)   Rastogi, R., Srivastava, A., and Dhawan, B.N. Effect of picroliv on impaired hepatic mixed function oxidase system in carbon tetrachloride-intoxicated rats. <u>Drug Dev Res</u> 41(1997) : 44-7.

(76)   Lissoni, P., et al. Physiopathology of IL-12 in human solid neoplasms: Blood levels of IL-12 in early or advanced cancer patients, and their variations with surgery and immunotherapy. <u>J Biol Regul Homeost Agents</u> 12(1998) : 38-41.

(77)   Thong-Ngam, D., et al. Diagnostic role of serum interleukin-18 in gastric cancer patients. <u>World J Gastroenterol</u> 12(2006) : 4473-7.

(78)   Tung, K.H., et al. Serum interleukin-12 levels in alcoholic liver disease. <u>J Chin Med Assoc</u> 73(2010) : 67-71.

(79)   Tangkijvanich, P., Thong-Ngam, D., Mahachai, V., Theamboonlers, A., and Poovorawan, Y. Role of serum interleukin-18 as a prognostic factor in patients with hepatocellular carcinoma. <u>World J Gastroenterol</u> 13(2007) : 4345-9.

(80)   Li, J., et al. Cytokine and autoantibody patterns in acute liver failure. <u>J Immunotoxicol</u> 7(2010) : 157-64.

(81)   Koizumi, F., Kawamura, T., Ishimori, A., Ebina, H., and Satoh, M. Plasma paracetamol concentrations measured by fluorescence polarization immunoassay and gastric emptying time. <u>Tohoku J Exp Med</u> 155(1988) : 159-64.

APPENDICES

APPENDIX A

Descriptives: AST

Group	N	Mean	Std. Deviation	Std. Error	95% Confidence Interval for Mean		Minimum	Maximum
					Lower Bound	Upper Bound		
Control	8	86.1250	6.89591	2.43807	80.3599	91.8901	77.00	96.00
APAP	8	583.2500	118.30197	41.82606	484.3471	682.1529	443.00	736.00
APAP + CUR 200	8	197.3750	14.39184	5.08828	185.3431	209.4069	174.00	215.00
APAP + CUR 600	8	111.3750	8.33131	2.94556	104.4099	118.3401	103.00	127.00
Total	32	244.5313	210.87024	37.27694	168.5044	320.5581	77.00	736.00

ANOVA: AST

	Sum of Squares	df	Mean Square	F	Sig.
Between Groups	1278217.844	3	426072.615	119.019	.000
Within Groups	100236.125	28	3579.862		
Total	1378453.969	31			

APPENDIX A (Continue)

Multiple comparisons: AST

(I) Group	(J) Group	Mean Difference (I-J)	Std. Error	Sig.	95% Confidence Interval Lower Bound	95% Confidence Interval Upper Bound
Control	APAP	-497.12500[*]	29.91597	.000	-578.8049	-415.4451
	APAP + CUR 200	-111.25000[*]	29.91597	.005	-192.9299	-29.5701
	APAP + CUR 600	-25.25000	29.91597	.833	-106.9299	56.4299
APAP	Control	497.12500[*]	29.91597	.000	415.4451	578.8049
	APAP + CUR 200	385.87500[*]	29.91597	.000	304.1951	467.5549
	APAP + CUR 600	471.87500[*]	29.91597	.000	390.1951	553.5549
APAP + CUR 200	Control	111.25000[*]	29.91597	.005	29.5701	192.9299
	APAP	-385.87500[*]	29.91597	.000	-467.5549	-304.1951
	APAP + CUR 600	86.00000[*]	29.91597	.036	4.3201	167.6799
APAP + CUR 600	Control	25.25000	29.91597	.833	-56.4299	106.9299
	APAP	-471.87500[*]	29.91597	.000	-553.5549	-390.1951
	APAP + CUR 200	-86.00000[*]	29.91597	.036	-167.6799	-4.3201

*. The mean difference is significant at the 0.05 level.

Tukey HSD[a]

Group	N	Subset for alpha = 0.05 1	Subset for alpha = 0.05 2	Subset for alpha = 0.05 3
Control	8	86.1250		
APAP + CUR 600	8	111.3750		
APAP + CUR 200	8		197.3750	
APAP	8			583.2500
Sig.		.833	1.000	1.000

Means for groups in homogeneous subsets are displayed.

a. Uses Harmonic Mean Sample Size = 8.000.

APPENDIX B

Descriptives: ALT

Group	N	Mean	Std. Deviation	Std. Error	95% Confidence Interval for Mean		Minimum	Maximum
					Lower Bound	Upper Bound		
Control	8	42.6250	6.94751	2.45631	36.8167	48.4333	36.00	59.00
APAP	8	186.0000	43.72969	15.46078	149.4411	222.5589	139.00	255.00
APAP + CUR 200	8	65.2500	3.10530	1.09789	62.6539	67.8461	61.00	70.00
APAP + CUR 600	8	47.5000	4.72077	1.66905	43.5533	51.4467	41.00	54.00
Total	32	85.3438	63.31876	11.19328	62.5149	108.1726	36.00	255.00

ANOVA: ALT

	Sum of Squares	df	Mean Square	F	Sig.
Between Groups	110339.844	3	36779.948	73.837	.000
Within Groups	13947.375	28	498.121		
Total	124287.219	31			

APPENDIX B (Continue)

Multiple comparisons: ALT

(I) Group	(J) Group	Mean Difference (I-J)	Std. Error	Sig.	95% Confidence Interval	
					Lower Bound	Upper Bound
Control	APAP	-143.37500*	11.15931	.000	-173.8434	-112.9066
	APAP + CUR 200	-22.62500	11.15931	.202	-53.0934	7.8434
	APAP + CUR 600	-4.87500	11.15931	.972	-35.3434	25.5934
APAP	Control	143.37500*	11.15931	.000	112.9066	173.8434
	APAP + CUR 200	120.75000*	11.15931	.000	90.2816	151.2184
	APAP + CUR 600	138.50000*	11.15931	.000	108.0316	168.9684
APAP + CUR 200	Control	22.62500	11.15931	.202	-7.8434	53.0934
	APAP	-120.75000*	11.15931	.000	-151.2184	-90.2816
	APAP + CUR 600	17.75000	11.15931	.400	-12.7184	48.2184
APAP + CUR 600	Control	4.87500	11.15931	.972	-25.5934	35.3434
	APAP	-138.50000*	11.15931	.000	-168.9684	-108.0316
	APAP + CUR 200	-17.75000	11.15931	.400	-48.2184	12.7184

*. The mean difference is significant at the 0.05 level.

Tukey HSDa

Group	N	Subset for alpha = 0.05	
		1	2
Control	8	42.6250	
APAP + CUR 600	8	47.5000	
APAP + CUR 200	8	65.2500	
APAP	8		186.0000
Sig.		.202	1.000

Means for groups in homogeneous subsets are displayed.

a. Uses Harmonic Mean Sample Size = 8.000.

APPENDIX C

Descriptives: GSH

Group	N	Mean	Std. Deviation	Std. Error	95% Confidence Interval for Mean		Minimum	Maximum
					Lower Bound	Upper Bound		
control	8	10.1725	.10607	.03750	10.0838	10.2612	9.91	10.21
APAP	8	2.7525	.15526	.05489	2.6227	2.8823	2.64	2.94
APAP+CUR200	8	9.1550	.48642	.17197	8.7483	9.5617	8.70	9.61
APAP+CUR600	8	9.7225	.22321	.07892	9.5359	9.9091	9.61	10.21
Total	32	7.9506	3.08289	.54498	6.8391	9.0621	2.64	10.21

ANOVA: GSH

	Sum of Squares	df	Mean Square	F	Sig.
Between Groups	292.378	3	97.459	1.212E3	.000
Within Groups	2.252	28	.080		
Total	294.631	31			

APPENDIX C (Continue)

Multiple comparisons: GSH

(I) Groop	(J) Group	Mean Difference (I-J)	Std. Error	Sig.	95% Confidence Interval Lower Bound	95% Confidence Interval Upper Bound
control	APAP	7.42000*	.14181	.000	7.0328	7.8072
	APAP+CUR200	1.01750*	.14181	.000	.6303	1.4047
	APAP+CUR600	.45000*	.14181	.018	.0628	.8372
APAP	control	-7.42000*	.14181	.000	-7.8072	-7.0328
	APAP+CUR200	-6.40250*	.14181	.000	-6.7897	-6.0153
	APAP+CUR600	-6.97000*	.14181	.000	-7.3572	-6.5828
APAP + CUR 200	control	-1.01750*	.14181	.000	-1.4047	-.6303
	APAP	6.40250*	.14181	.000	6.0153	6.7897
	APAP+CUR600	-.56750*	.14181	.002	-.9547	-.1803
APAP + CUR 600	control	-.45000*	.14181	.018	-.8372	-.0628
	APAP	6.97000*	.14181	.000	6.5828	7.3572
	APAP+CUR200	.56750*	.14181	.002	.1803	.9547

*. The mean difference is significant at the 0.05
level.

Tukey HSD

Group	N	Subset for alpha = 0.05 1	2	3	4
APAP	8	2.7525			
APAP+CUR200	8		9.1550		
APAP+CUR600	8			9.7225	
control	8				10.1725
Sig.		1.000	1.000	1.000	1.000

Means for groups in homogeneous subsets are displayed.

APPENDIX D

Descriptives: MDA

Group	N	Mean	Std. Deviation	Std. Error	95% Confidence Interval for Mean		Minimum	Maximum
					Lower Bound	Upper Bound		
control	8	1.4512	.01458	.00515	1.4391	1.4634	1.43	1.47
APAP	8	3.5500	.05398	.01909	3.5049	3.5951	3.51	3.64
APAP+CUR200	8	1.4725	.00886	.00313	1.4651	1.4799	1.46	1.48
APAP+CUR600	8	1.4638	.00518	.00183	1.4594	1.4681	1.46	1.47
Total	32	1.9844	.91881	.16242	1.6531	2.3156	1.43	3.64

ANOVA: MDA

	Sum of Squares	df	Mean Square	F	Sig.
Between Groups	26.148	3	8.716	1.079E4	.000
Within Groups	.023	28	.001		
Total	26.170	31			

APPENDIX D (Continue)

Multiple comparisons: MDA

(I) Group	(J) Group	Mean Difference (I-J)	Std. Error	Sig.	95% Confidence Interval	
					Lower Bound	Upper Bound
control	APAP	-2.09875*	.01421	.000	-2.1376	-2.0599
	APAP+CUR200	-.02125	.01421	.454	-.0601	.0176
	APAP+CUR600	-.01250	.01421	.815	-.0513	.0263
APAP	control	2.09875*	.01421	.000	2.0599	2.1376
	APAP+CUR200	2.07750*	.01421	.000	2.0387	2.1163
	APAP+CUR600	2.08625*	.01421	.000	2.0474	2.1251
APAP+CUR200	control	.02125	.01421	.454	-.0176	.0601
	APAP	-2.07750*	.01421	.000	-2.1163	-2.0387
	APAP+CUR600	.00875	.01421	.926	-.0301	.0476
APAP+CUR600	control	.01250	.01421	.815	-.0263	.0513
	APAP	-2.08625*	.01421	.000	-2.1251	-2.0474
	APAP+CUR200	-.00875	.01421	.926	-.0476	.0301

Tukey HSD

Group	N	Subset for alpha = 0.05	
		1	2
control	8	1.4512	
APAP+CUR600	8	1.4638	
APAP+CUR200	8	1.4725	
APAP	8		3.5500
Sig.		.454	1.000

Means for groups in homogeneous subsets are displayed.

APPENDIX E

Descriptives: IL-12

Group	N	Mean	Std. Deviation	Std. Error	95% Confidence Interval for Mean		Minimum	Maximum
					Lower Bound	Upper Bound		
control	8	7.0850	1.39843	.49442	5.9159	8.2541	4.51	9.05
APAP	8	29.1613	3.33950	1.18069	26.3694	31.9531	24.86	33.35
APAP+CUR200	8	11.6063	1.67913	.59366	10.2025	13.0100	9.63	13.70
APAP+CUR600	8	9.6275	1.37548	.48630	8.4776	10.7774	7.65	11.02
Total	32	14.3700	9.05287	1.60034	11.1061	17.6339	4.51	33.35

ANOVA: IL-12

	Sum of Squares	df	Mean Square	F	Sig.
Between Groups	2415.855	3	805.285	180.767	.000
Within Groups	124.735	28	4.455		
Total	2540.590	31			

APPENDIX E (Continue)

Multiple comparisons: IL-12

(I) Group	(J) Group	Mean Difference (I-J)	Std. Error	Sig.	95% Confidence Interval	
					Lower Bound	Upper Bound
control	APAP	-22.07625*	1.05532	.000	-24.9576	-19.1949
	APAP+CUR200	-4.52125*	1.05532	.001	-7.4026	-1.6399
	APAP+CUR600	-2.54250	1.05532	.098	-5.4239	.3389
APAP	control	22.07625*	1.05532	.000	19.1949	24.9576
	APAP+CUR200	17.55500*	1.05532	.000	14.6736	20.4364
	APAP+CUR600	19.53375*	1.05532	.000	16.6524	22.4151
APAP+CUR200	control	4.52125*	1.05532	.001	1.6399	7.4026
	APAP	-17.55500*	1.05532	.000	-20.4364	-14.6736
	APAP+CUR600	1.97875	1.05532	.261	-.9026	4.8601
APAP+CUR600	control	2.54250	1.05532	.098	-.3389	5.4239
	APAP	-19.53375*	1.05532	.000	-22.4151	-16.6524
	APAP+CUR200	-1.97875	1.05532	.261	-4.8601	.9026

*. The mean difference is significant at the 0.05 level.

Tukey HSD

Group	N	Subset for alpha = 0.05		
		1	2	3
control	8	7.0850		
APAP+CUR600	8	9.6275	9.6275	
APAP+CUR200	8		11.6063	
APAP	8			29.1613
Sig.		.098	.261	1.000

Means for groups in homogeneous subsets are displayed.

APPENDIX F

Descriptives: IL-18

Group	N	Mean	Std. Deviation	Std. Error	95% Confidence Interval for Mean		Minimum	Maximum
					Lower Bound	Upper Bound		
control	8	29.1662	3.72467	1.31687	26.0523	32.2802	22.14	33.81
APAP	8	1.3952E2	15.58665	5.51071	126.4905	152.5520	115.71	160.95
APAP+CUR200	8	53.4688	18.17085	6.42437	38.2775	68.6600	38.57	82.28
APAP+CUR600	8	35.2075	2.17656	.76953	33.3879	37.0271	31.90	38.33
Total	32	64.3409	46.48709	8.21783	47.5806	81.1013	22.14	160.95

ANOVA: IL-18

	Sum of Squares	df	Mean Square	F	Sig.
Between Groups	62850.397	3	20950.132	141.619	.000
Within Groups	4142.139	28	147.934		
Total	66992.536	31			

APPENDIX F (Continue)

Multiple comparisons: IL-18

(I) Group	(J) Group	Mean Difference (I-J)	Std. Error	Sig.	95% Confidence Interval	
					Lower Bound	Upper Bound
control	APAP	-110.35500*	6.08140	.000	-126.9591	-93.7509
	APAP+CUR200	-24.30250*	6.08140	.002	-40.9066	-7.6984
	APAP+CUR600	-6.04125	6.08140	.754	-22.6454	10.5629
APAP	control	110.35500*	6.08140	.000	93.7509	126.9591
	APAP+CUR200	86.05250*	6.08140	.000	69.4484	102.6566
	APAP+CUR600	104.31375*	6.08140	.000	87.7096	120.9179
APAP+CUR200	control	24.30250*	6.08140	.002	7.6984	40.9066
	APAP	-86.05250*	6.08140	.000	-102.6566	-69.4484
	APAP+CUR600	18.26125*	6.08140	.027	1.6571	34.8654
APAP+CUR600	control	6.04125	6.08140	.754	-10.5629	22.6454
	APAP	-104.31375*	6.08140	.000	-120.9179	-87.7096
	APAP+CUR200	-18.26125*	6.08140	.027	-34.8654	-1.6571

*. The mean difference is significant at the 0.05 level.

Tukey HSD

Group	N	Subset for alpha = 0.05		
		1	2	3
control	8	29.1662		
APAP+CUR600	8	35.2075		
APAP+CUR200	8		53.4688	
APAP	8			1.3952E2
Sig.		.754	1.000	1.000

Means for groups in homogeneous subsets are displayed.

APPENDIX G

**PATHOLOGY REQUEST FORM
DEPARTMENT OF PATHOLOGY
KING CHULALONGKORN MEMORIAL HOSPITAL**

Name………………………………………Age…………………Sex……………...
HN…………………Ward……………Date of operation……………....................
Attending physician………..Code…………………..Pager/phone…………………….
Clinical History…………………………………………………………………………..
…………………………………………………………………………………………….....
....
....
....
....
Investigations……………………………………………………………………….......
....
....
Clinical Diagnosis……………………………………………………………………..…
Type of operation…………………………………………………………………………
REQUEST FOR…

Surgical Pathology	**amount of container**
❑ PA001 Routine histopathology, < 2 cm	…………………....
❑ PA002 Routine histopathology, > 2 cm	……………………
❑ PA003 Bone marrow biopsy	…………………....
❑ PA008 Kidney biopsy (Routine)	……………………
❑ PA004 Kidney biopsy (Complete study)	……………………
❑ PA005 Liver biopsy	…………………....
❑ PA006 Transplant pathology	……………………
❑ PA007 Frozen section biopsy	……………………
❑ PA028 Others……………….	…………………....
Cytology	
❑ PA009 Pap smear	…………………....
❑ PA010 Fine needle aspiration	……………………
❑ PA011 Exfoliative cytology	……………………
(sputum, cavity fluid, etc.)	
❑ PA012 Others………………..	……………………
❑ **Electron Microscopy**	
❑ PA013 TEM	……………………
PA014 SEM	……………………
Histochemistry	
❑ PA015 AFB	
❑ PA016 Giemsa	
❑ PA017 GMS	
❑ PA018 Mucin	
❑ PA019 Others………………..	

APPENDIX G (Continue)

Immunohistochemistry
- ❏ PA021   Immunofluorescence
- ❏ PA022   Breast cancer markers
- ❏ PA023   Lymphoma/Leukemia typing
- ❏ PA024   Soft tissue tumor typing
- ❏ PA029   Complete immunohistochemical study
- ❏ PA025   Others………………...
- ❏ PA026   **Autopsy**
- ❏ PA027   **Other hospital**…………

SPECIMEN DATA (Type of specimen, anatomic site, side, size, amount, etc.)

Total number of containers or slides………………………………………………………

Container No. 1……………………………………….Amount or size……………...

Container No. 2……………………………………….Amount or size……………...

BIOGRAPHY

NAME: Miss Kanjana Somanawat
STUDENT ID: 52 748624 30
BIRTHDAY: June 28, 1987
PLACE OF BIRTH: House No. 48, Village No. 9, Thakhanon sub-district, Khiri Rat Nikhom district, Surat Thani, 84180
EDUCATION
DEGREE: Bachelor of Science (B. Sc.)
MAJOR: Biomedical Sciences
FACULTY: Science
NAME OF INSTITUTION: Rangsit University
YEAR OF GRADUATION: 14 October 2009
PUBLICATION: Somanawat, K., Thong-Ngam, D., and Klaikeaw, N. Effects of curcumin attenuated hepatitis in mice with paracetamol overdose. Thai J Gastroenterol 13(2012) : 43-49.